

Results from the Coin et al. (1992, 1994) studies indicates no difference between deposition in central or peripheral regions of the lung. They also confirm that chrysotile splits longitudinally in the lungs with a half-life that is competitive with the clearance rates measured in this study. Clearance was found to be very length-dependent, so that rates decrease from a half-life of about 10 days for fibers about 4 μm in length, through 30 days for fibers 8 μm , to 112 days (which is no different from zero) for fibers longer than 16 μm (all after adjusting for longitudinal splitting). Importantly, the brief follow-up period (30 days) is too short to provide an adequate evaluation of the longer term clearance pools observed in other studies and certainly too short to evaluate any effects potentially associated with chrysotile dissolution. Also, that the decay curves for clearance were limited to four points, makes evaluation of the slopes for these curves highly uncertain.

Coin et al. (1992, 1994) also report that the mass of chrysotile deposited during these short exposures (i.e., no more than 20 μg) is very small compared to levels at which overload has been reported to occur (approximately 1 mg, see, for example, Yu and Yoon 1991) and that the volume of the 16 μm fibers, which have an average diameter of 0.2 μm and therefore a mean volume of 0.5 μm^3 , is small relative to the volume at which macrophage clearance of non-fibrous particles is reported to be hindered (Morrow 1988). Thus, the authors conclude that fiber length presents an additional constraint on macrophage clearance, independent of any other overload. They also indicate that inhibition of clearance due to fiber length is independent of fibrosis.

Coin et al. (1992, 1994) also discuss the effect of fibrosis on clearance. They indicate that, although increased concentrations of short fibers are observed in focal areas of fibrosis, it is more likely that such fibers accumulate because clearance is hindered by fibrosis in these areas than the hypothesis that the short fibers are causing fibrosis. This is because, as they point out, there are too many studies demonstrating the lack of ability of short fibers to induce fibrosis.

Evidence in the Coin et al. (1992, 1994) studies suggests that no translocation from central to peripheral regions of the lung were detected. An upper bound rate that is about 20% of clearance is reported. However, the short follow-up time in this study would have precluded slower processes from being detected. Despite the lack of evidence of translocation, the authors report that duct bifurcations in peripheral regions of the lung where fibers are deposited are no more than 1–2 mm from the visceral pleura. In fact, in the 1994 study, the authors show that 50% of the primary duct bifurcations in the peripheral portion of the rat lung occur within 1 mm of the visceral pleura and some occur as close as 220 μm . Deposited fibers may also affect the pleura by inducing generation of diffusible, inflammatory agents.

A short-term inhalation study by Warheit et al. (1997) evaluated retention of chrysotile and aramid fibers. In this study, rats (and hamsters) were exposed, nose only, for 6 hours/day, 5 days/week for 2 weeks by inhalation to UICC chrysotile and p-aramid fibers (each at two doses of 460 or 780 fibers/ml, although the size range of these fibers is not stated nor is the manner in which they were analyzed). Fixed lungs were digested in chlorox during preparation for asbestos analysis. Animals were followed for up to a year post-exposure.

As in studies described above, results from the Warheit et al. (1997) study indicate rapid clearance of short chrysotile fibers, but slow to non-existent clearance of fibers longer than 20 μm . In contrast, aramid fibers apparently degrade and are subsequently cleared fairly rapidly

in vivo. Based on the data provided in figures, although the reported concentrations of chrysotile and aramid fibers to which animals were exposed were equivalent, at both the lower and higher concentrations, it appears that rats initially retain 3 to 5 times as many aramid fibers as chrysotile fibers (at least for the size range counted, which was not reported). For both fiber types, clearance appears rapid for an initial period of approximately 90 days post-exposure. During this time, the mean length of chrysotile fibers also appears to increase steadily, which suggests rapid, preferential clearance of short structures. After the initial period, it appears that (as the authors suggest), a residual concentration of longer fibers are cleared only very slowly, if at all.

Oberdorster et al. (1988) instilled a 3 ml suspension of irradiated amosite into the bronchio-alveolar space of the right diaphragmatic lobe of the lungs of dogs to evaluate clearance and transport. The amosite used was modified by sedimentation from UICC amosite to contain only fibers shorter than 20 μm . One dog also had unmodified UICC amosite instilled directly into a lymph node in the thigh. The dogs had been cannulated to allow collection of lymph from the right lymph duct-RLD and the thoracic duct-TD (both in the neck).

Results from Oberdorster et al. (1988) indicate that within 4 hours following instillation in the lung, low activity was noted in postnodal lung lymph, but not in either the RLD or TD. Within 24 hours, however, activity and fibers (determined by SEM) were observed in both the RLD and the TD. The median length of fibers observed in the lymph were significantly longer than the instilled material, although there appeared to be a cutoff length of 16 μm in fibers observed at nodes and 9 μm in fibers observed directly in lymph. Fibers recovered from lymph were also significantly thinner and appeared to exhibit an absolute cutoff at a maximum width of 0.5 μm . Fibers recovered from the TD and RLD in the dog that had unmodified UICC amosite instilled directly into leg lymph were all short (with a maximum length of 6 μm). Since collection times were all short, the authors indicate that it is unknown whether longer fibers would have been observed at later times. The authors also note the almost total absence of fibers shorter than 1 μm in lymph, which they assume are cleared rapidly and efficiently by alveolar macrophages.

Oberdorster et al. (1988) also report that a rough calculation, based on the fraction of the material originally instilled that was recovered in the first 24 hours, it would take approximately 6 years to clear all of the instilled asbestos (assuming no other clearance mechanisms were active).

Everitt et al. (1997) performed a short-term inhalation study that is interesting, particularly, because it focused on pleural (as opposed to lung) fiber burden. The authors exposed rats and hamsters to one type of refractory ceramic fiber (RCF-1) by nose-only inhalation for periods of 0, 4, and 12 weeks and animals were held for observation for up to an additional 12 weeks post-exposure. Exposures were conducted for 4 hours/day, 5 days/week, at $45.6 \pm 10 \text{ mg/m}^3$. Groups of 6 animals were held for 0, 4, 12, and 24 weeks to determine pleural fiber burden. An agarose casting method was reportedly used to recover fibers from the pleura. Analysis was by electron microscopy. Fibers were observed in the pleura at each time point examined (including samples from rats sacrificed immediately following the last day of a 5-day exposure). Fibers were all reported to be short and thin (geometric mean length: 1.6 μm with GSD: 1.8, geometric mean diameter: 0.1 μm with GSD: 1.5). Concentrations averaged approximately 40,000 fibers (per whole pleura, units not reported). The authors indicate that such fibers would not typically be

visible by optical microscopy. They also indicate that use of casts may be a more efficient method of recovering fibers from the pleura.

Everitt et al. (1997) indicate that observation of rapid translocation of short, thin fibers to the pleura has also been observed in studies of chrysotile so these results are not unique. Although it is stated that the mechanisms facilitating translocation are currently unknown, the authors indicate that their finding of site-specific mesothelial proliferation supports observations by Boutin et al. (1996) that asbestos fibers accumulate in the parietal pleura of humans at sites associated with lymphatic drainage. Kane and MacDonald (1993) have suggested that fibers are transported to these locations by pleural macrophages. However, the mechanisms by which fibers are transported from the lung to the pleura are still unconfirmed.

Older Retention Studies. Although the older retention studies generally support the results of newer studies (such as those cited above), older studies are sometimes limited by such things as the tracking of lung burden in terms of fiber mass or use of analytical techniques such as infrared spectroscopy for detection of asbestos, which are neither capable of distinguishing individual fibers nor provide any information on their sizes. Tracking of lung burdens in terms of mass may not reflect the fate of long, thin fibers, which (by increasing concurrence) appear to be the legitimate focus of studies evaluating biological hazards attributable to asbestos.

In two studies (Roggli and Brody 1984 and Roggeli et al. 1987), Roggeli and coworkers tracked the behavior of chrysotile (not UICC) and UICC crocidolite in rats following 1 hour exposure by inhalation to 3.5–4.5 mg/m³ dusts. The authors indicate that this results in deposition of approximately 21 µg of dust. Portions of the lower lung lobes of selected rats were collected and digested for asbestos analysis using a scheme that was shown to be representative. To evaluate size distributions, more than 400 fibers from each sample were characterized by SEM. Fiber dimensions were then used to estimate total fiber mass.

Based on their study, Roggeli and coworkers indicate that similar fractions of inhaled chrysotile and crocidolite dust are deposited in the lung during inhalation (23 and 19%, respectively). The authors therefore concluded that respirability and deposition do not depend on fiber type. Importantly, however, the manner in which this study was conducted does not facilitate distinguishing deposition in the deep lung from deposition in the upper respiratory tract.

Roggeli and coworkers further indicate that clearance rates for the two fiber types appear comparable. Of the chrysotile initially deposited, they report that 81% of this material is cleared after 4 weeks. Similarly, 75% of the crocidolite is cleared. Importantly, because this is based on total mass (estimated by summing volume contributions from observed fibers), it may not reflect the specific behavior of long, thin structures. Therefore, it is difficult to compare such results with those of more recent studies. However, the authors do report that short structures are cleared more readily than long structures and that chrysotile is observed to split longitudinally *in vivo* (based on observation that the total number of chrysotile structures initially increases and the mean length increases). The authors further conclude that clearance rates appear to be independent of fiber type.

In another short-term study, Kauffer et al. (1987) report that the average length of retained chrysotile structures increases in rat lungs following 5-hours inhalation of chrysotile dust. Based

on their results, the authors report that fibers shorter than approximately 8 μm are preferentially cleared. Kauffer and coworkers also confirm that chrysotile fibers split longitudinally in the lung. In fact, several other studies (Kimizuka et al. 1987; Le Bouffant 1980) also provide supporting observations that chrysotile fibers (or bundles) split longitudinally in the lung.

In two studies (Morgan et al. 1978, 1980), Morgan and coworkers report on the fate of fibers following short-term inhalation of radio-labeled fibers by rats. In the first study (Morgan et al. 1978), rats inhaled UICC anthophyllite at 35 mg/m³ for a total of 8.4 hours spread over 3 days. The authors report that the rats retained approximately 190 μg of dust at the end of exposure, mostly in the alveolar region; the authors assumed that conducting airway clearance is sufficiently rapid to clear this portion of the lung within a few days. Beginning about 7 days following exposure, the rats were then sacrificed serially for a period up to 205 days following exposure. Because anthophyllite fibers are relatively thick, fibers were analyzed by optical microscopy. Fibers were determined both in free cells (mostly macrophages) recovered in bronchopulmonary lavage and in lung tissue. Tissue samples and cells were digested in KOH and peroxide in preparation for fiber analysis.

Based on this first study, Morgan et al. (1978) report that anthophyllite lung content declined steadily by a process that could be described as a simple first order decay with a half-life of approximately 76 days. Free macrophages recovered by lavage, initially contained about 8 pg and this too declined steadily with a half-life of about 49 days. The authors further indicate that, if the number of macrophages remains constant with time (i.e., they are replaced at the same rate they are cleared), then the decay of the load in the macrophages should match what is observed in the rest of the lung. They suggest that the discrepancy may be due either to an influx of an increasing number of macrophages in response to injury with time and/or to transfer of some fibers through the alveolar wall. They also cite unpublished work indicating that uptake of fibers by alveolar macrophages is essentially complete within hours after cessation of exposure.

The authors also report that, initially, the lengths of fibers recovered in lung lavage was greater than in the original aerosol, but that the prevalence of the longest fibers decreased after the first 7 days. In lung tissue, however, the fraction of longer fibers (among total fibers) steadily increased with time. This suggests rapid clearance of naked fibers by muco-ciliary transport (which is a length independent process) with later times dominated by slower clearance in the deep lung by alveolar macrophages, which is a length-dependent process.

Morgan and coworkers also radiometrically determined the fraction of fibers in rat feces (prior to sacrifice). They assumed that after 14 days, this would represent the fraction of asbestos cleared primarily from the alveolar region of the lung. Initially 1.4% of lung anthophyllite content was excreted daily, but this fell to 0.5% after 120 days. The authors indicate that this suggests that the elimination from asbestos in lung tissue cannot be described by a single exponential because multiple processes are involved and that, over longer periods of time, the slower processes become increasingly important.

In the second study, Morgan et al. (1980) track the fate of several size-selected radiolabeled glasses in rats, again following short-term inhalation. From an analysis of the size dependence of deposited fibers in this study, the authors suggest that alveolar deposition in the rat is limited to structures with aerodynamic equivalent diameters less than about 6 μm and that deposition in

this region of the lung falls precipitously for fibers with thicknesses between about 2 and 3 μm (aerodynamic equivalent diameter). For fibers that are the density of asbestos, this represents an upper bound limit to alveolar deposition for the absolute thickness of a fiber of approximately 1.5 μm with fibers deposition of fibers thicker than approximately 0.7 μm being drastically reduced. This is in concordance with conclusions concerning deposition provided in Section 6.1.4. Alveolar deposition efficiency is also shown to decrease with increasing fiber length, at least for fibers longer than approximately 8 μm , also in concordance with findings presented in Section 6.1.4.

Intratracheal Instillation. The fate of fibers following intratracheal instillation into the lungs has also proven informative in some studies. For example, Wright and Kuschner (1975) intratracheally instilled paired samples each of several types of glass fibers, fluoramphibole, and crocidolite into guinea pigs. For each mineral tested, a sample with predominantly short structures (25 mg total dose for crocidolite, reportedly 99% <5 μm) and another with predominantly long structures (4 mg total dose for crocidolite, reportedly 80% >10 μm) were evaluated. Unfortunately, the authors do not report how fibrous structures were characterized. Results in the cited paper report observations only after 2 years following the last injection.

Wright and Kuschner (1975) report that long structures uniformly caused fibrosis (primarily involving the respiratory bronchioles and alveoli and abutting the terminal bronchioles) while the short structures were uniformly phagocytized and generally removed to thoracic lymph nodes. Among other things, clearance to lymph suggests that fibers reached the interstitium (Section 6.2.5). It is interesting that, even after 2 years of recovery, the authors observe elevated levels of macrophages in the alveoli of animals dosed with short structures. Based on the relative size distributions of the samples analyzed, the authors report that structures up to 10 μm in length appear to be efficiently scavenged by macrophages. Based on the observation of larger numbers of short structures than expected in comparison with their fractions in the original samples, the authors further conclude that glass structures underwent biodegradation so that longer structures broke down into shorter structures that could be phagocytized.

Wright and Kuschner (1975) also report that long fibers are occasionally visible within the fibrotic interstitium of dosed animals. The long-fiber dosed animals also show macrophages in hilar lymph nodes containing fibers that are too small to resolve and all of them are short. In short-fiber dosed animals, some fibers are seen to remain in the lung within aggregates of macrophages, both in alveoli and the interstitium. Short-fiber dosed animals also show many more macrophages within the hilar lymph nodes than long-fiber dosed animals.

In two reports of the same study (Bellman et al. 1986, 1987), Bellman and coworkers followed the fate of UICC chrysotile, UICC crocidolite, several fibrous glasses, and other manmade mineral fibers following a single intratracheal instillation of 0.3 ml of fibrous material in rats. Groups of rats were then sacrificed at 1, 6, 12, 18, and 24 months following instillation. Lungs were low temperature ashed and the resulting, filtered suspension analyzed by transmission electron microscopy. Some of the fiber types were also acid treated with 0.1 M oxalic acid for 24 hours prior to instillation.

Bellman and coworkers (1987) report that short fibers (<5 μm) from all of the fiber types were shown to be cleared from the lungs with half-lives of approximately 100 days, with the asbestos

varieties tending to exhibit slightly longer half-lives than the other fibers. Short crocidolite fibers exhibited a half-life of 160 days. The half-life for clearance of short chrysotile was reported to be 196 days (the longest of all). However, this was attributed to positive contributions from breakage of longer fibers.

Bellman and coworkers (1987) report that the behavior of the different long fibers ($>5 \mu\text{m}$) for the different fiber types was radically different. The authors report no observed net decline in long crocidolite fibers over the 2 years of follow-up. They also report no observable changes in width of these fibers with time. In contrast, long chrysotile fibers increased in number with time throughout the 18-month follow-up period and this was attributed to longitudinal splitting. The width of these fibers reportedly decreased with time.

Bellman et al. (1987) also report that a more detailed examination of the time dependence of the width of chrysotile fibers indicates a rapid increase in the number of thin fibrils ($<0.05 \mu\text{m}$ in width) and thin bundles ($<0.1 \mu\text{m}$ in width) within 100 days (at the expense of thicker bundles). The authors suggest that this would result in rapid decrease in the number of chrysotile structures visible by optical microscopy and, possibly, increased clearance of the thinnest fibrils by dissolution, but this study shows no increased rate of clearance for thinner chrysotile structures compared to thicker structures (when viewed by electron microscopy). In contrast, long chrysotile fibers that were acid-leached prior to instillation reportedly disappeared with a half-life of 2 days.

Generally, the rate of clearance of the long fractions of the other fibers reported in the Bellman et al. (1986, 1987) papers varies as a function of solubility and overall thickness. Importantly, all half-lives are reported to have high standard errors in this study, due to the small number of animals included for examination.

In summation, virtually all short-term retention studies indicate that:

- fibers retained in the lung tend to be shorter and thinner than the aerosols from which they derive and the size distributions of retained structures tend to be more similar overall than the size distributions observed in the original aerosols;
- chrysotile asbestos undergoes rapid, longitudinal splitting in the lung while amphiboles do not;
- by mass, chrysotile and amphibole asbestos are deposited in the lung with comparable efficiencies, although it is not clear whether chrysotile dusts tend to contain sufficient numbers of curly fibers to limit deposition in the deep lung;
- multiple clearance processes operate over different time frames and some of these processes are strongly length-dependent. Fibers shorter than approximately $10 \mu\text{m}$ appear to be cleared rapidly relative to longer fibers and those longer than approximately $20 \mu\text{m}$ are not cleared efficiently at all (if the fibers are insoluble). The Bellman et al. (1986, 1987) studies appear to contrast with other studies in this regard in that they suggest fibers longer than $5 \mu\text{m}$ do not readily clear;

- the quickest clearance process (presumably muco-ciliary clearance) is not dependent on length; and
- the effects of fiber diameter on clearance have not been well delineated overall, although fibers that reach the deep lung appear to be largely limited to those thinner than approximately 0.7 μm .

These findings are in addition to those mentioned previously from the newer studies:

- multiple clearance mechanisms (operating over multiple time scales) contribute to clearance;
- for sufficiently soluble fibers, long fibers clear more rapidly than short fibers;
- for insoluble fibers, a subset of long fibers clears rapidly while the remaining long fibers clear only extremely slowly, if at all;
- short fibers of all types are cleared at approximately the same rate (much more rapidly than long, insoluble fibers);
- a small fraction of short fibers may be retained for long periods under certain circumstances (sequestered in alveolar macrophages) despite overall rapid clearance of these structures; and
- there is some suggestion that short asbestos fibers clear somewhat more slowly than short fibers of the other, non-asbestos mineral types studied.

Regarding specifically the clearance of long fibers, it appears that a component of all such fibers clears rapidly within the first 2 weeks and this likely represents muco-ciliary clearance. A second component (representing as much as 60% of the fibers) clears within 90 days and this likely represents clearance by alveolar macrophages. The remaining long fibers are cleared only very slowly, if at all, and this likely represents fibers that are sequestered in granulomas or that escape into the interstitium.

6.2.1.2 *Studies involving chronic or sub-chronic exposures*

Although the results of older retention studies following longer term (sub-chronic or chronic) exposure were difficult to reconcile with the results following shorter-term exposures, newer studies suggest greater consistency and a clearer picture of the fate of fibers in the lung. Moreover, although there are further suggestions of mineralogy (fiber type) dependent effects with some clearance mechanisms, it is important that size effects be considered simultaneously, if the dynamics of these processes are to be understood.

In some of the latest studies, for example, Hesterberg et al. (1993, 1995, and 1998b) exposed rats (nose only) by inhalation to a series of man-made vitreous fibers (including a variety of fibrous glasses, rock wools, and refractory ceramic fibers) and two kinds of asbestos: chrysotile (intermediate length NIEHS fiber) and crocidolite (size selected). Animals were dosed for 6

hours/day, 5 days/week for up to 2 years at target concentrations of 10–60 mg/m³. The target concentration for chrysotile and crocidolite was 10 mg/m³. Animals were periodically sacrificed during the exposure regimen to determine the character of the retained fibers. Vitreous fiber aerosols were characterized by PCM, SEM or, for chrysotile, by TEM. The right accessory lung lobe of sacrificed animals was tied off, frozen, and stored for lung burden analysis.

For analysis, lung lobes were dried to constant weight, ashed, the residue suspended in distilled water, and then filtered on Millipore filters (for examination by optical microscopy) or Nuclepore filters (for analysis by SEM or TEM for chrysotile). Approximately 100 fibers were reportedly characterized to establish fiber size distributions. However, this is problematic for this study because chrysotile asbestos concentrations in the aerosols to which the animals were exposed contained approximately 100 times as many fibers as the other aerosols. Thus, although no fibers longer than 20 µm were observed during characterization of the chrysotile, the concentration of such long fibers could still have been larger in this aerosol than the other aerosols and it would not necessarily have been observed. This is also true of lung burden analyses especially because indirect preparation tends to magnify the number of short chrysotile structures observed in a sample.

A comparison of the retention patterns of chrysotile and RCF-1 from the Hesterberg et al. (1998b) study is particularly instructive. First, it should be noted that, in contrast to the values reported by the authors of this study, chrysotile and RCF-1 in fact appear to exhibit comparable *in vitro* dissolution rates (12.7 vs. 8 ng/cm²·hr, respectively) when rates are measured using comparable techniques (see discussion in Section 6.2.4). The dissolution rates quoted in the Hesterberg et al. study are not derived in comparable studies.

Although a full set of time-dependent analyses are apparently not available for chrysotile, it is reported that approximately 14% of those chrysotile WHO fibers observed to be retained after 104 days of exposure continue to be retained after 23 days of recovery. Under the same conditions, it is reported that 43% of RCF-1 fibers are retained, which suggests more rapid clearance for chrysotile. Even adjusted for the fraction of RCF-1 structures that are longer than 20 µm (and that are presumably cleared even more slowly), approximately 37% of the RCF-1 WHO fibers (<20 µm) are apparently retained over this period, which is still more than twice the rate reported for chrysotile. Still, more detailed characterization of the size distributions of these two fiber types would need to be evaluated before it could be concluded with confidence that chrysotile is cleared more rapidly than RCF-1 or that dissolution plays a role. In fact, dissolution would tend to cause more rapid clearance only of the longest fibers (i.e., the ones that cannot be cleared by macrophages [see Section 6.2.1.1]), which would further reduce the apparent retention rate of the shorter RCF fibers, making it even more comparable to the chrysotile number.

Based on these studies, Hesterberg et al. (1998b) report that fibers deposited and retained in the lung tend to be shorter and thinner on average than the sizes found in the original aerosol. It is also apparent from their data that long RCF-1 fibers clear more rapidly than short RCF-1 fibers (although a small fraction of long structures are retained at all time points following a recovery period after cessation of exposure), which is consistent with observations in other studies for fibers that dissolve at moderate rates. In the short-term study performed by the same laboratory, Hesterberg et al. (1998a), long fiber (>20 µm) RCF-1a appears to clear at approximately the

same rate as the shorter structures ($<5\text{ }\mu\text{m}$), although the scatter in the data (and an unexplained initial rise in long-fiber RCF) prevent a more careful comparison. Similar results are also apparent in the data presented for MMVF21. It should be noted that the dissolution rates for RCF-1 and MMVF21 bracket the estimated dissolution rate for chrysotile asbestos (when the three are derived from comparable studies [see Section 6.2.4]).

The data presented in Table 3 of Hesterberg et al. (1998b), which are reproduced in Table 6-3, can also be used to evaluate the time-trend of retention during chronic exposure. The values presented in Columns 2, 4, and 6 of Table 6-3 present, respectively, measurements of the lung burden for chrysotile WHO fibers, RCF-1 WHO fibers, and RCF-1 long WHO fibers ($>20\text{ }\mu\text{m}$) in animals sacrificed immediately following cessation of exposure for the time period indicated in Column 1. Unlike results reported in some earlier chronic studies based on mass (see below), there is no evidence from this table (based on fiber number) that chrysotile lung burdens reach a plateau. Rather chrysotile lung burdens (as well as RCF-1 lung burdens) continue to increase with increasing exposure.

The data presented in Table 6-3 can also be used to gauge the relative efficiency with which the chrysotile and RCF fibers are retained. Considering that the number of fibers inhaled (N_{inh}) over the period of exposure would be equal to the product of the aerosol concentration (C_{air} in f/cm^3), the breathing rate of the exposed animal (R_B in cm^3/week), and time (in weeks):

$$N_{inh} = C_{air} * R_B * t \quad (\text{Eq. 6-1})$$

and the efficiency of retention is simply equal to the quotient of the number of fibers retained (N_{lung}) and the total number inhaled: N_{lung}/N_{inh} , then the efficiency of retention is estimated by the following simple relationship:

$$\text{Efficiency of retention} = N_{lung}/(C_{air} * R_B * t) \quad (\text{Eq. 6-2})$$

By rearranging Equation 6-2, one obtains:

$$\text{Efficiency of retention} * t = (N_{lung}/(C_{air} * R_B)) \quad (\text{Eq. 6-3})$$

Table 6-3. Fraction of Fibers Retained Following Chronic Exposure^a

Exposure Period	Chrysotile		RCF-1			
	WHO Fibers	Lung/Aerosol Ratio	WHO Fibers	Lung/Aerosol Ratio	Long WHO fibers	Lung/Aerosol Ratio
Weeks	f/lung x 10 ⁶					
0.0357			0.009	4.81E-05	0.002	1.98E-05
13	250	0.024	39	0.209	3	0.030
26	180	0.017	56	0.299	6	0.059
52	1020	0.096	119	0.636	20	0.198
78	853	0.080	173	0.925	21	0.208
104	1600	0.151	143	0.765	25	0.248
Aerosol Concentration						
(f/ml)	10600		187		101	

^aSource: Hesterberg et al. (1998b)

Because the breathing rate for the rats in the Hesterberg et al. (1998b) study can be considered a constant for all experiments, Equation 6-3 indicates that the slope of a plot of N_{lung}/C_{air} versus time should yield estimates of the relative efficiency of retention for each of the fiber types evaluated. The plot for chrysotile is presented in Figure 6-3. Results from this plot and similar plots for RCF-1 WHO fibers and long WHO fibers (data not shown), result in the following estimates of the relative efficiencies of retention (along with the corresponding R^2 value for the fit of the linear trend line):

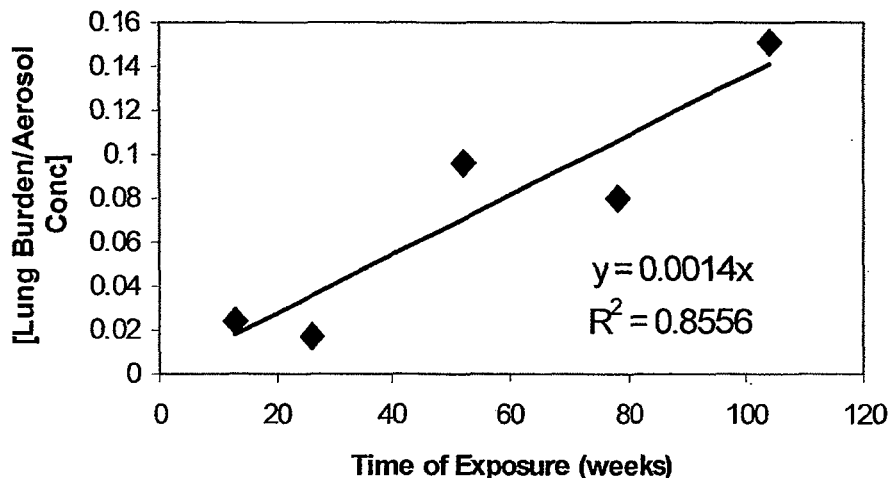
$$\text{chrysotile WHO fibers: } 0.0014, R^2=0.856$$

$$\text{RCF-1 WHO fibers: } 0.0095, R^2=0.694$$

$$\text{RCF-1 long, WHO fibers: } 0.0026, R^2=0.880$$

Thus, it appears that chrysotile WHO fibers are retained somewhat less efficiently than either RCF-1 WHO fibers or RCF-1 long WHO fibers. However, whether this is due to less efficient deposition or more efficient clearance cannot be determined from this analysis. It is also not possible to determine whether such differences are due to the effects of differences in size distributions among the various fiber types. Interestingly, based on the data presented by Hesterberg et al., which indicates that long RCF-1 WHO fibers clear more rapidly than regular RCF-1 WHO fibers, the differences in the relative retention of these two length categories of fibers is due primarily to relative efficiency of clearance.

Figure 6.3:
[Chrysotile Lung Burden/Aerosol Concentration] vs. Time of Exposure



In a similar study involving chronic exposure to Syrian golden hamsters (Hesterberg et al. 1997), fiber retention and biological effects associated with exposure to amosite and a series of MMVF's were evaluated. The amosite was size selected and hamsters were exposed to one of three levels (0.8 ± 0.2 , 3.7 ± 0.6 , and 7.3 ± 1.0 mg/m³). Amosite lung burdens were shown to increase regularly with dose and time of exposure. The time dependence for accumulation of some of the MMVF's was more complicated. None of the animals were apparently followed for any recovery periods following cessation of exposure. The authors also indicate that the severity of the effects observed (inflammation, cellular proliferation, fibrosis, and eventually several mesotheliomas), appear to correlate well with the concentration of fibers longer than 20 μ m.

Earlier Studies. Earlier studies, in which asbestos concentrations tend to be monitored as total mass tend commonly to show that chrysotile asbestos is neither deposited as efficiently as various amphibole asbestos types nor is it retained as long (i.e., it is cleared much more rapidly from the lungs). In fact, several such studies tend to show that chrysotile asbestos concentrations eventually reach a plateau despite continuing exposure, which suggests that clearance and deposition come into balance and a steady state is reached. In contrast, amphibole asbestos concentrations continue to rise with increasing exposure, even at the lowest exposure levels at which experimental animals have been dosed. Such observations do not appear to be entirely consistent with those reported in newer studies (see above) that track fiber number concentrations (in specific size categories). In these newer studies, chrysotile retention is not observed to level off, but continues to increase in a manner paralleling amosite or other fibers. As indicated below, however, the limitations associated with these older studies suggest that,

although it may not be easy to reconcile them quantitatively with the newer studies, results from these studies are not necessarily inconsistent with those of the newer studies. Moreover, the trends observed in the newer studies are likely more directly relevant to issues associated with the induction of asbestos-related disease. The problems with the older studies are:

- the trends seen in the older studies (based on mass) may mask the more important trends associated with deposition and retention of long, thin fibers. Thus, results from such studies may not be directly relevant to considerations of risk; and
- the observed differences between chrysotile and the amphiboles may be attributed to differences in size distribution (among other possibilities). Thus, lacking detailed information on size distributions, it is difficult to reconcile the results from the older studies with results from the newer studies, which explicitly track specific size ranges of fibers.

Given these limitations, the earlier studies are only mentioned briefly.

Middleton et al. (1979) tracked the fate of asbestos (as mass measured by infrared spectroscopy) in rats following inhalation of several asbestos aerosols (UICC chrysotile A, UICC amosite, and UICC crocidolite) at multiple concentrations (reported at 1, 5, or 10 mg/m³). To account for possible differences in the nocturnal (vs. daytime) activity level of rats, several groups of rats were also exposed in a “reversed daylight” regimen (in which cages were darkened during the real day and bathed in light during the real night). Acclimatized rats in these groups were thus dosed at times corresponding to their night. Exposure continued for 7 hours/day, 5 days/week, for 6 weeks.

Results from the Middleton et al. (1979) study were fit to a three compartment model (originally proposed by Morgan et al. 1978) and the authors concluded that clearance was independent of fiber type, but that the initial deposition of fibers was very dependent on fiber type. This was indicated by a “K-factor” representing the efficiency of initial deposition. Chrysotile showed K factors that range between 0.17 and 0.36 and vary inversely with the initial exposure concentration. In contrast, amosite exhibits a K factor of 0.69 and crocidolite a K factor of 1.0 and both are independent of exposure level. Although the design of this experiment precluded fitting of the shortest two compartments of the model (with half-lives of 0.33 and 8 days, from Morgan et al. (1978), they did optimize the half-life of the longest compartment. Fibers in this compartment were cleared with a half-life of 170 days.

In a series of studies, Davis and coworkers (1978, 1980, 1988a, and 1988b) report that retention of asbestos (measured in terms of mass) appears to be a function of fiber type and surface charge in addition to fiber size. With regard to fiber type, for example, Davis et al. (1978) report that substantially more amphibole (amosite) asbestos appears to be deposited and retained in the lungs of exposed rats than chrysotile. Chrysotile is also apparently cleared more readily than amosite. However, mineralogical effects should only be judged after adjusting for fiber size.

Rats in the studies by Davis and coworkers were dosed at 6 hours/day, 5 days/week for up to 1 year at dust concentrations of 2, 5, or 10 mg/m³ (depending on the specific experiment). Right lungs (used for determining lung burden) were ashed and the residue was washed in distilled

water and filtered. The residue was formed into a potassium bromide disc and asbestos (mass) content was determined by infrared spectroscopy.

Jones et al. (1988) report that the lung-tissue concentration of amosite increases continually with exposure (at 7 hours/day, 5 days/week for up to 18 months) and the rate of increase is proportional to the level of exposure. A leveling off of amphibole concentrations in lung tissue was not observed in this study as long as exposure continued, even for the lowest level of exposure (0.1 mg/m^3) studied. The lowest exposure concentration evaluated in this study is only 1% of the concentration at which chrysotile lung burdens were shown to reach equilibrium in other retention studies (see below). Importantly, however, these are only the older studies in which fiber burden is tracked by mass. The newer studies don't show this effect.

The authors also report lack of any apparent change in size distribution with time among the fibers recovered from the animal's lungs, which suggests lack of substantial clearance even of short fibers. However, the longest recovery period following the cessation of exposure evaluated in this study is only 38 days, which may be too short to allow evidence for differential clearance as a function of size to become apparent (at least in a chronic study; the time dependence in chronic studies such as this are more complicated than for short-term studies). Moreover, the apparent inclusion of lymph nodes as part of the lung homogenate may have caused short fibers initially cleared from the lung to be added back in. In this study, lungs were recovered intact including the associated mediastinal and hilar lymph nodes, which were ashed in toto. Ash residue was washed in acid and water, ultrasonicated and filtered for electron microscope analysis. Note that such a procedure would include any fibers cleared to local lymph nodes.

In a widely cited study, Wagner et al. (1974), report that amphibole lung burdens increase continually as long as exposure to amphiboles continues and that amphibole concentrations in lung tissue decrease only slowly following cessation of exposure. In contrast, chrysotile lung burdens reach a plateau despite continued exposure. Importantly, asbestos content was estimated by determining total lung silica content and adjusting for similar analysis on filtered samples of the original aerosols. Thus, in addition to suffering from the limitations associated with tracking fiber burden by mass, there are questions concerning the validity of using total silica to represent asbestos content. Therefore, for these reasons and the additional reason of the lack of controlling for fiber size, the ability to interpret this study and reconcile its conclusions with those of newer studies is severely limited.

Chronic Inhalation of Non-fibrous Particulate Matter. A recent study involving chronic inhalation of non-fibrous materials is helpful at elucidating the relative localization of particles in rats and primates. Nikula et al. (1997) studied lung tissue from a 2-year bioassay, in which Cynomolgus monkeys and F344 rats were exposed to filtered, ambient air or air containing one of three particulate materials: diesel exhaust (2 mg/m^3), coal dust (2 mg/m^3 , particles $<7 \mu\text{m}$ in diameter), or a 50/50 mix of diesel exhaust and coal dust (combined concentration: 2 mg/m^3).

Results from Nikula et al. (1997) indicate that responses to all three particulate materials were similar. The particles tended to localize in different compartments of the lung in a species-specific manner:

- 73% of particles remain in the alveolar lumen of rats, but only 43% in monkeys. The remainder can be found in the interstitium;
- in both the alveolar lumen and in the interstitium, virtually all of the particles are observed to be isolated within macrophages; and
- the particles in the interstitium reside in macrophages within the alveolar septa, the interstitium of respiratory bronchioles, the adventitia and lymphatic capillaries surrounding arterioles and veins of pulmonary parenchyma, or in the pleura.

It is not known whether free particles penetrate the epithelial lining of the airway lumena and escape into the interstitium or whether such particles are first engulfed by macrophages and then transported in their macrophage "hosts" into the interstitium.

Importantly, even after 2 years of exposure, the particles in the interstitium do not appear to have elicited a tissue response. Also, the aggregates of particle-laden macrophages observed in alveolar lumena elicited significantly less of a tissue response in monkeys than in rats. Such responses included: alveolar epithelial hyperplasia, inflammation, and focal septal fibrosis.

The authors further indicate that "epithelial hyperplasia concomitant with aggregation of particle-laden macrophages in alveolar lumen is a characteristic response to many poorly soluble particles in the rat lung, both at exposure concentrations that result in lung tumors and at concentrations below those resulting in tumors. Such a response, however, was not characteristic of what was observed in monkeys. Among other things, these differences in responses suggest that rats may not represent a good model for human responses to inhalation of poorly soluble particulate matter. It would also have been interesting had they tested a "benign" dust such as TiO₂.

In summation:

- results of (newer) sub-chronic and chronic retention studies are generally consistent with those of retention studies that track lung burden following short-term exposure (Section 6.2.1.1);
- there is some indication in these sub-chronic and chronic studies that chrysotile asbestos may not be retained as efficiently as amphibole asbestos. It is likely, however, that such distinctions are due more to fiber size than fiber type so that definitive conclusions concerning such effects cannot be reached until better studies that properly account for both size and type are conducted; and
- although earlier studies that track mass instead of fiber number suggest otherwise, chrysotile and amphibole asbestos concentrations (when measured by fiber number) continue to increase with time as long as exposure continues. Due to a lack in the ability to distinguish among size-dependent effects when lung burdens are tracked by mass, the results of the earlier studies are not necessarily inconsistent with the results of the later studies.

6.2.2 Animal Histopathological Studies

Studies in which the lungs of dosed animals are examined to determine the fate and effects of inhaled asbestos are helpful for understanding the movement and distribution of retained particles within the lung and surrounding tissue. Both the newest retention studies and the older retention studies tend to include at least some of this type of information. They also tend to indicate a consistent picture of the fate and effects of asbestos. While such studies tend to confirm that translocation in fact occurs, they are less helpful for elucidating the specific mechanisms by which translocation occurs.

Newer Studies. Ilgren and Chatfield (1998) studied the biopersistence of three types of chrysotile ("short chrysotile" from Coalinga in California, "long" Jeffrey fiber from the Jeffrey mine in Asbestos, Quebec, and UICC-B (Canadian) Chrysotile, a blend from several mines in Quebec). Both the Coalinga-fiber and the Jeffrey-fiber were subjected to further milling prior to use. In this study, rats were exposed via inhalation for 7 hours/day, 5 days/week for up to 2 years. Concentrations were: $7.78 \pm 1.46 \text{ mg/m}^3$ for Coalinga-fiber, $11.36 \pm 2.18 \text{ mg/m}^3$ for Jeffrey-fiber, and $10.99 \pm 2.11 \text{ mg/m}^3$ for the UICC-B fiber. An additional group of rats was also dosed for a single 24-hour period with Jeffrey-fiber at a concentration of $5,000 \text{ f/ml} > 5 \mu\text{m}$. Estimates of lung content of chrysotile were based on measurements of total silica content. The character of the three chrysotile types evaluated in this study was previously reported (Campbell et al. 1980; Pinkerton et al. 1983). The animal studies were conducted previously with the overall approach reported by McConnell et al. (1983a,b) and Pinkerton et al. (1984). Based on the characterization presented in these papers, Coalinga-fiber is short, but not as extremely short as suggested by the authors:

Ratio of fibers longer than:	5 μm :	10 μm :	20 μm
Coalinga-fiber:	200:	78:	0.98
Jeffrey-fiber:	591:	220:	78

Such calculations also suggest that the single, "high" dose in this experiment was equivalent only to a concentration that is approximately 10 times the other concentrations studied, so that it is equivalent only to a 10-day exposure and small relative to the longer term (up to 2 years) exposures considered in this study.

Results reported by Ilgren and Chatfield (1998) indicate that the lung burden for short fiber chrysotile initially increases with exposure, reaches a steady state, and then decreases steadily following cessation of exposure. Approximately 95% of this material is cleared within 2 years. Thus, short fibers appear to exhibit the trend suggested by the older chronic retention studies that tracked burden by mass and is consistent with the newer studies indicating rapid clearance of short structures (Section 6.2.1.2).

In the studies reported by Ilgren and Chatfield (1998), most short fibers are found initially within alveolar macrophages and, while concentrations in Type I epithelium, interstitial cells, and interstitial matrix increase with time, little appears to be taken up by Type II epithelium. Small

amounts of short fiber chrysotile are also observed to be taken up by endothelial cells. There is also little sign of inflammation or fibrosis following exposure to the Calidria-chrysotile.

Jeffrey-chrysotile also initially appears to be taken up primarily by alveolar macrophages, but later becomes most prevalent in the interstitial matrix and, to a lesser extent, in interstitial cells. Substantial numbers of fibers are also taken up by Type I epithelium and small amounts by endothelial cells. Similar, but slightly delayed effects were seen for UICC-B chrysotile (which has a smaller fraction of long fibers and therefore, the authors suggest, takes longer to accumulate). Note that, by 12 months, the majority of long fibers from both these types were found in interstitial matrix while the majority of Calidria-material was still found in alveolar macrophages. This is consistent with observations concerning behavior between short and long fibers reported by Wright and Kushner (1975), Section 6.2.1.1. At this point, the Jeffrey-material also caused substantial thickening of the basement membrane and most fibers in the interstitium were trapped within the collagenous matrix. The authors note that some of the most severe interstitial changes occurred adjacent to areas of bronchiolar metaplasia. Such effects were not seen with Calidria-exposure.

Thickened basement membranes, calcium deposits, metaplastic changes, and structural abnormalities were all observed with long fiber exposure, but not with Calidria-exposure. Interstitial macrophages also showed morphological changes following phagocytosis of fibers. While Calidria-material was about evenly distributed between interstitial matrix and cells, the vast majority of long fiber material was found in the matrix. Movement into the matrix was also observed to increase even after exposure ceased. With time, the number of long fibers in interstitial cells declined modestly, but declined precipitously for Calidria-material.

Jeffrey-fibers accumulated in Type I epithelial cells during exposure and then levels decreased slowly after exposure ceased. UICC-B fibers accumulated more slowly, never reaching the same levels as for Jeffrey and decreased more rapidly. Concentrations of Calidria-fibers in Type I epithelial cells was low at all time points.

Type II epithelial cells accumulated very few fibers of any type (although they took up slightly more Jeffrey-fiber than the others). All three fiber types caused substantial increases in interstitial cells (mostly macrophages) at 3 months and this increase persisted for the Jeffrey-fiber, but decreased to background after 24 months for the other two fiber types. Fibroblast numbers also increased with the long fiber types, but not Calidria-chrysotile.

Type II epithelial cells showed decreases in volume and number that persisted until exposure to long fiber ceased and these cells displayed dramatic structural aberrations despite absence of a fiber load. One possible explanation for the observed changes in Type II cells, especially the reduction in their number, is that they were undergoing terminal differentiation to Type I cells (see Section 4.4). In fact, the apparent absence of fibers observed within Type II cells might be explained by such cells taking up fibers, but being induced to terminally differentiate, once fibers are accumulated. Overall, Type II cells displayed greater cellular response than Type I cells (which might also suggests a role for cytokines). All effects were observed to be fiber length dependent and all were exaggerated following exposure to long fiber material.

Rats exposed to long fiber had numerous accumulations of dust-laden interstitial macrophages and/or small focal accumulations of dust within the interstitium at the end of the lifetime study, but such changes were not observed for Calidria-exposed animals.

The lung burden for rats exposed to the single, "high" Jeffrey-fiber exposure (based on total silica) at 12 months (i.e., 12 months post-exposure) was not different from controls. Therefore, the authors conclude that short-term, "high" exposures are rapidly cleared (even exposures containing substantial quantities of long fibers). Other changes induced by the single, short-term high exposure of Jeffrey-fiber that was followed for 24 months also showed reversion to close to background status. Importantly, these observations are not based on quantitation of fiber burden in lung tissue. Rather they are inferred by observing the effects caused by the presence of fibers. This may suggest, for example, that more than 10 day's worth of exposure would be required at this level of exposure before irreversible lesions develop.

In the study by Hesterberg et al. (1997), which was previously discussed (Section 6.2.1.2), the authors note (among dosed hamsters) that the magnitude of cellular effects appeared to differ among the fibrous glasses as a function of their relative biodurability. For animals dosed with the least biopersistent glass, only transient effects (influx of macrophages, development of microgranulomas) were observed and these did not progress further. For the more persistent glasses, injury progressed through more intense inflammation, interstitial fibrosis, pleural collagen deposition, mesothelial hypertrophy and hyperplasia and eventually, mesothelioma. The authors also suggest that amosite appears to be more potent than chrysotile, even when aerosols contain comparable numbers of fibers longer than 20 μm .

Choe et al. (1997) exposed rats to chrysotile and crocidolite (both NIEHS samples) by inhalation for 6 hours/day, 5 days/week, for 2 weeks. The rats were then sacrificed and their pleural cavities lavaged. Results indicate that significantly more pleural macrophages were recovered in pleural lavage fluid at one and 6 weeks following exposure than sham exposed rats. The centrifuged pellet from pleural lavage fluid from one of four rats also exhibited long ($>8 \mu\text{m}$), thin ($<0.5 \mu\text{m}$) crocidolite fibers (1 week following exposure). The concentration of fibers in this pellet suggested approximately 1 f per 4,000 cells in the pleura. Note that chrysotile rats were not examined for fiber content.

Older Studies. In the series of studies by Davis et al. (1978, 1980, 1985, 1986a), the authors generally report similar histopathological observations that emphasizes a marked distinction between effects from long and short fibers. From the 1986 study, for example, Davis et al. report that at the end of 12 months of exposure, rats exposed to long fibers (amosite in this case) exhibited deposits of granulation tissue around terminal and respiratory bronchioles. They further indicate that the granulation tissue consists primarily of macrophages and fibroblasts with occasional foreign body giant cells.

As the animals aged, there was increased evidence of collagen deposits in these lesions and the oldest lesions consist mainly of acellular, fibrous tissue. The alveolar septa in these older animals showed progressive thickening. Initially, this was apparently due primarily to hyperplasia of Type II epithelial cells, but with time was increasingly due, first, to reticulin and, later, to collagenous deposits in the septal walls. Asbestos dust was frequently visible in these deposits. Epithelial cells lining alveoli adjacent to the oldest lesions also tended to become

cuboidal in shape. As the animals aged, these areas of interstitial fibrosis became more extensive.

In contrast, animals exposed to short fibers (also amosite in this case) showed no such lesions (peribronchial fibrosis) at any point in time. At the end of exposure, the lungs of these animals contained large numbers of pulmonary macrophages packed with fibers, but these cells remained free in the alveolar spaces. The authors report that large numbers of laden macrophages sometimes aggregated in alveoli close to respiratory bronchioles, but that there would be no formation of granulation tissue or thickening of alveolar septa at these locations. Thus, with the exception of the presence of dust-laden macrophages, the structure of the lung of these rats was not altered.

In the Davis et al. (1987) study of chrysotile, a slight variation of the above scenario is worth noting. In this study, the development of peribronchial fibrosis was reported for animals dosed both with the long fiber material and with the short fiber material. However, the authors also report that the short fiber chrysotile in this study in fact contains a sizable fraction of longer structures and this finding was corroborated by more formal size characterization (Berman et al., unpublished) later conducted in support of a study to evaluate the effects of size (Berman et al. 1995).

In this study, Davis et al. also reported observations on the morphological changes observed in the mesothelium during these studies. The authors indicate that the older animals in these studies exhibit "areas of vesicular pleural metaplasia consisting of loose, fibrous tissue containing large vesicular spaces lined with flattened cells". The authors also report that examination in previous studies indicates that these cells are of a mesothelial type.

Davis et al. report that, "...occasionally the walls between vesicular spaces were so thin that they consisted of two closely opposed layers of extended and flattened cells with no basement membrane in between them. Where cells were supported by areas of fibrous tissue, a basement membrane was present. While no method for the direct quantification of this pleural metaplasia has been developed, its occurrence is closely related to the presence of advanced interstitial fibrosis or adenomatosis in the lung tissue and it is particularly common where patches of this type of parenchymal lesion have reached the surface. It is not known whether such lesions are precursors to mesothelioma. Davis et al. also note that neither of the two mesotheliomas observed in this study showed histological patterns consistent with the observed vesicular hyperplasia.

Brody et al. (1981) tracked the distribution of chrysotile following inhalation by rats. Asbestos was initially deposited almost exclusively at alveolar duct bifurcations. In agreement with Pinkerton et al. (1986), the degree of deposition appeared to be an inverse function of the path length and bifurcation number for each alveolar duct. Uptake by macrophages and type 1 epithelial cells were observed following deposition. Asbestos was observed both in lipid vesicles and free in the cytoplasm of type 1 cells. After 8 days, alveolar duct bifurcations became thickened with an influx of macrophages. Asbestos was also observed in basement membrane below the epithelium. Apparently, structures had been transported through type 1 cells to the basement membrane. Once in the basement membrane, asbestos may enter the interstitium. Predominantly short structures were monitored in this study. Long structures were

not readily observed (but this is likely a counting problem; under such circumstances, short structures may serve as surrogates for the presence of other structures).

Intratracheal Instillation. Bignon et al. (1979) studied the rate of translocation of various materials in rats. Chrysotile, crocidolite, and glass fibers were intrapleurally injected into rats and their concentration was monitored as a function of time in lung parenchyma and other tissues removed from the pleura. Within 1 day following injection, asbestos was detectable in lung parenchyma. After 90 days, asbestos was found in all of the tissues analyzed. Based on the rate of translocation to the lung, crocidolite migrates about 10 times more rapidly than chrysotile (on a mass basis). The rate of migration of glass is in between the two asbestos types. Structures initially found in the lung were significantly shorter than the average size of structures injected. After 7 months, however, the average lengths of structures in all tissues monitored were longer than the average length of structures originally injected. Thus, short structures migrate more rapidly than longer structures (possibly by a different mechanism), but long structures eventually translocate as well. Within a target tissue, preferential clearance of short structures also contributes to observed increases in the average length of the structures with time.

Studies of Non-Fibrous Particulate Matter. Studies of the fate and effects of respirable, non-fibrous particulate matter provide evidence for at least one mechanism by which particles (and fibers) may be transported to the interstitium.

Li et al. (1997) evaluated the effect of urban PM 10, carbon black, and ultrafine carbon black on rats following intratracheal instillation (0.2 ml volume instilled containing between 50 and 125 µg of particles). After 6 hours, there was a noted influx of neutrophils (up to 15% of total cells observed in bronchioalveolar lavage–BAL fluid) and increases in epithelial permeability was surmised based on increased total protein (including increases in levels of lactate dehydrogenase, which is a marker for cell membrane damage) in BAL fluid.

Conclusions. Overall, observations among both the newer and the older studies (including the study by Wright and Kuschner 1975, see Section 6.2.1.2) tend to be highly consistent, particularly with regard to the distinction between the effects of short and long fibers. Typically, long fibers initially produce substantial inflammation characterized by an influx of macrophages and other inflammatory cells. Ultimately, exposure to such fibers cause thickening of alveolar septa (particularly near avleolar duct bifurcations) due to a combination of epithelial hyperplasia and deposition of reticulin and, later, collagen resulting in interstitial fibrosis. In contrast, short fibers cause an initial influx of macrophages and, long-term, show persistent accumulations of fiber-laden macrophages both in alveolar lumena and in pulmonary lymph nodes, but otherwise no structural changes are observed in the lung tissue of these animals.

These studies also provide ready evidence of the effects of fiber translocation, but generally offer only limited evidence for elucidating the mechanisms by which such translocation occurs. There is evidence that Type I (and possibly Type II) epithelium phagocytize particles and fibers and it is possible that such fibers may be passed through to the basement membrane and the interstitium. For Type I cells, the distance between the alveolar lumen and the basement membrane averages less than 1 µm in any case (Section 4.4). Certainly fibers are also observed in the interstitium. Particulate studies also indicate that oxidative stress induced by particulate matter and fibers may cause morphological changes in Type II cells with consequent loss of

integrity of the epithelium, which increases its permeability overall and may also allow diffusional passage of particles and fibers.

6.2.3 Human Pathology Studies

Human pathology studies provide additional information concerning the nature of asbestos deposition, clearance, and retention. These are the studies in which lung burdens are measured in samples of lung tissue and correlated with the exposures received by the individuals from which the lung samples derive.

Among the advantages of human pathology studies is that they provide direct insight into the behavior of asbestos in humans. They are also limited, however, by the lack of ability to obtain time-dependent estimates of lung burden (because samples are derived from deceased individuals), by the manner in which lung tissue is stored (several of the fixatives employed to store tissue samples have been shown to enhance dissolution of asbestos (Law et al. 1990, 1991), by the manner in which samples are prepared for asbestos analysis, by the manner in which asbestos is analyzed, and by the limited ability to re-construct the uncontrolled exposures experienced by study subjects (Section 5.2).

Perhaps most importantly, the ability to construct anything but the coarsest quantitative comparisons across subjects is also typically limited by use of "opportunistic" tissue samples (i.e., use of samples that happened to have been collected and stored during autopsy or necropsy) because such samples are not controlled for location on the respiratory tree (i.e., the linear distance and branch number from the trachea) that is represented by the sample. Because it has previously been shown that deposition is a strong function of such location (see, for example, Yu et al. 1991), comparisons across lung samples not controlled for these variables are problematic. It has also been shown that samples collected from adjacent locations in lung parenchyma can in fact exhibit strikingly different fiber concentrations due specifically to the differences in the location of the respiratory tree represented by the alveoli and respiratory bronchioles in the spatially adjacent samples (Brody et al. 1981; Pinkerton et al. 1986 [Section 5.2]).

Despite the above indicated cautions, when interpreted carefully, human pathology studies can provide useful evidence regarding fiber deposition, clearance, and retention in the human lung.

Newer Studies. Among the most recent studies, Finkelstein and Dufresne (1999) evaluated trends in the relationship between lung burdens for different fiber types and different size ranges as a function of historical exposure, the duration of such exposure, the time since last exposure, and other variables. The analyses were performed among 72 cases from which tissue samples could be obtained (including 36 asbestosis cases, 25 lung cancer with asbestosis cases, and 11 mesothelioma cases).

Due to the excessive scatter in the data, most of the analyses presented depend on "Lowess Scatterplot Smoothers". Moreover, although not stated, it is likely that the tissue samples obtained were "opportunistic" in that they were not matched or controlled for relative position in the respiratory tree.

Finkelstein and Dufresne (1999) employed the multi-compartment model developed by Vincent et al. (1985) to evaluate trends in their data. The features of this model include:

- a compartment representing conducting airways that are cleared within minutes to hours by muco-ciliary transport;
- a compartment representing the subset of fibers reaching the pulmonary portion of the lung that are cleared by alveolar macrophages and transported to the muco-ciliary escalator. This type of clearance is also considered relatively rapid with half-lives of no more than several days to several weeks. Macrophage clearance is also considered size-dependent and long fibers are cleared less efficiently than short fibers;
- when sufficient dust is inhaled (or dust is sufficiently cytotoxic) to impair the motility of macrophages (either by volumetric overload or by toxicity), a sequestration compartment forms that consists of laden, but immobile, macrophages. Although this compartment may ultimately be cleared to lymphatic drainage, such clearance is assumed to be slow and size dependent (with half-lives of 2 or 3 years for short fibers and 8 years for fibers longer than 10 μm); and
- once the macrophage system is overloaded, fibers may cross the alveolar epithelium and reach the interstitium and this compartment must be cleared by transport to lymphatic drainage, which is assumed to be an extremely slow process.

Finkelstein and Dufresne (1999) indicate that chrysotile splits both longitudinally and transversely in the lung and that chrysotile lung burdens decrease significantly with time since last exposure (with short fibers clearing even faster than long fibers), while tremolite burdens do not appear to decrease with time since last exposure. They also suggest that smoking does not appear to affect clearance rates.

Finkelstein and Dufresne (1999) indicate that these type of studies are not useful for examining the behavior in rapidly clearing compartments of the lung, but they may provide insight concerning the more slowly clearing compartments. Based on their modeling, they suggest that tremolite is transferred to the sequestration compartment at rates that are 6–20 times that of chrysotile (which they indicate is comparable to what was found for crocidolite by de Klerk). The authors suggest that retained chrysotile concentrations tend to plateau after accumulation of about 35 years of exposure, while tremolite concentrations continue to increase. They also suggest, however, that chrysotile concentrations may begin to increase again after 40 years (suggesting the overload is eventually reached for chrysotile as well). Reported half-lives from the long-term compartment are:

Chrysotile

fibers shorter than 5 μm	3.8 years
fibers 5–10 μm in length	5.7 years
fibers longer than 10 μm	7.9 years

Tremolite

fibers shorter than 5 μm	14.3 years (not different from ∞)
fibers 5–10 μm in length	15.8 years (not different from ∞)
fibers longer than 10 μm	150 years (not different from ∞)

In a case-control study, Albin et al. (1994) examined the lung burdens of deceased workers from the asbestos-cement plant previously studied for mortality (Albin et al. 1990). In this study, details of the procedures used to prepare lung tissue for analysis were not provided. It is also assumed that available tissue samples were “opportunistic” in that they were not matched or controlled for relative position in the respiratory tree.

Results from Albin et al. (1994) are consistent with (but do not necessarily support) the hypothesis that chrysotile is cleared more readily from a long-term sequestration compartment than amphiboles. The authors also report that chrysotile fibers observed in this study are much shorter than the amphibole fibers observed, so that differences in clearance rates might be attributable to size differences. The authors also suggest that clearance is impaired by fibrosis.

Studies of Quebec Miners. Several authors also studied the lung content of various groups of deceased chrysotile miners in Quebec and found, despite overwhelming exposure to chrysotile from the ore (which contains only trace quantities of tremolite, see Case et al. 2000 and Sebastien et al. 1986), a substantial number of fibers (in some cases the majority of fibers) observed in the lungs of deceased miners from this area are tremolite. Thus, for example:

- in a study of lung burdens in 6 mesothelioma victims, Churg et al. (1984) showed that amphiboles structures were 5–15 times as plentiful as chrysotile despite the predominantly chrysotile exposure;
- in a study of lung tissue from 20 asbestosis cases, Pooley (1976) found substantial concentrations of tremolite in the lungs of deceased Quebec chrysotile workers;
- in a much larger study comparing lung burdens of Quebec workers with those from the South Carolina textile mill, which has also been extensively studied for asbestos-related mortality (Section 7.2.3), Sebastien et al. (1989) examined 161 lung tissue samples (89 from the Quebec mines). Results from this study indicate that geometric mean tremolite fiber concentrations were more than 3 times mean chrysotile fiber concentrations (18.4 vs. 5.3 f/ μg dry lung tissue) among the deceased Quebec miners evaluated. It was also found that, despite these differences, the overall size distributions of tremolite and chrysotile fibers observed in lung tissue were approximately the same, although this conclusion is suspect. A more detailed discussion of the results of this study is provided in Section 7.2.3; and

- in a more focused study using a subset of the lung samples evaluated by Sebastien et al. (1989), Case et al. (2000) found that the majority of long fibers (longer than 18 μm) in the lungs samples from the deceased Quebec miners that he examined were in fact composed of tremolite. These authors also found substantial concentrations of long tremolite fibers (relative to chrysotile fibers) in deceased workers from South Carolina and even higher concentrations of commercial amphibole fibers (amosite and crocidolite) in the lungs of these workers. Thus, in addition to suggesting the relative persistence of amphibole asbestos compared to chrysotile *in vivo*, this finding also suggests that the accepted notion that the South Carolina cohort studied by Dement et al. and McDonald et al. (see Appendix A) was exposed almost exclusively to chrysotile may not be correct. This study is discussed more fully in Section 7.2.3.

These observations provide evidence that either amphibole (tremolite) asbestos is deposited more efficiently in the compartments of the lung where clearance is slow or chrysotile asbestos is cleared more rapidly and efficiently from even the slowest clearing compartments of the lung (or both). Moreover, this conclusion appears to apply similarly to both short and long fibers.

In another study, McDonald et al. (1993) suggest more specifically that lung burden data from Quebec indicate little evidence of decreasing chrysotile concentration with time since last exposure. Rather they suggest simply that tremolite is initially deposited in the deep lung more efficiently. These authors also indicate that tremolite fibers are mostly optical while chrysotile are mostly "Stanton" or thinner.

McDonald et al. (1993) report good correlation of both tremolite and chrysotile with estimated past exposures, which contrasts with the findings of the evaluation we conducted on the data from Sebastien et al. (Section 7.2.3). In McDonald et al. (1985), reported geometric mean measurements for the various fibers in lung are: tremolite: 1×10^6 – 18.2×10^6 , chrysotile : 1.5×10^6 – 15.7×10^6 , respectively, when exposure varied from <30 mpcf to >300 mpcf. However, note that, if these are PCM measurements, this may not be telling the whole story. The authors also report that 66% of those who died 10 years since first exposure and half of those who died 30 years since first exposure showed high chrysotile concentrations in their lungs. Unfortunately, without access to the raw data from this study, it is not possible to identify the route of the apparent discrepancy between the findings of this study and those reported above for ostensibly similar studies.

Some of the pathology studies that have been published suggest that at least some clearance mechanisms show a dependence on fiber size, which is consistent with what is observed in animal studies (Section 6.2.1). Notably, for example, Timbrell (1982) studied deceased workers and relatives from the Paakkila anthophyllite mine in Finland. He found that structures shorter than 4 μm and less than 0.6 μm in diameter are completely cleared from healthy lungs. The efficiency of clearance decreases slowly with increasing size. Structures longer than 17 μm and thicker than 0.8 μm in diameter are not significantly cleared. The study is based on a comparison of structure size distributions in lungs compared to the structure size of the material in the original dust exposure. Timbrell also noted that asbestosis suppresses the removal process.

When considering the dependence of clearance on size (particularly via mechanisms involving phagocytosis), it is necessary to address differences in human and animal physiology. Due to differences in the morphology, for example, human macrophages have been shown capable of phagocytizing larger particles and longer fibers than macrophages found in mice and rats (Krombach et al. 1997 [for details, see Section 4.4]). Thus, the range of fibrous structures that are efficiently cleared from human lungs is expected to include longer fibers than the range efficiently cleared in mice or rats. Unfortunately, given the limited precision of the available data, the size ranges that are reported to be cleared efficiently in rats and humans, respectively, cannot be easily distinguished.

Several human pathology studies also support observations from animal studies indicating that clearance may be inhibited by the development of fibrosis (Albin et al. 1994; Churg et al. 1990; Morgan and Holmes 1980) or by heavy smoking. However, other studies do not indicate such hindered clearance either with smoking (Finkelstein and Dufresne 1999) or with fibrosis.

Older Studies. Morgan and Holmes (1980) examined tissue samples from 21 patients in England (10 who died of mesothelioma, 3 who died of lung cancer, and 8 who died of other causes). In this study, formalin-fixed tissue samples were digested with hypochlorite. The residue was then rinsed, diluted, and an aliquot filtered. The filter was mounted on a microscope slide and clarified for analysis by phase contrast optical microscopy. Importantly, the authors note that chrysotile fibers were ignored in this study because they would not generally have been detected by this technique. Portions of the filters were also carbon coated and prepared for TEM analysis. Based on the observation that only 19% of the fibers observed in this study were between 2.5 and 5 μm , when the authors expect airborne distributions to contain closer to 90% of the fibers within this size range, the authors conclude that short fibers are preferentially cleared from the lung. They also conclude, based on one subject with asbestosis whose lung tissue exhibited 72% short fibers, that asbestosis hinders clearance. The authors also note that fewer than 1% of ferruginous bodies (iron-coated asbestos bodies) are $<10 \mu\text{m}$ in length, which indicates (in agreement with previously published work) that such bodies seldom form on short fibers. They also suggest that virtually all fibers longer than 20 μm tend to be coated in the distributions they observe.

Le Bouffant (1980) studied the concentrations, mineralogy, and size distributions of asbestos fibers found in the lungs and pleura of deceased asbestos workers. Based on the analysis, Le Bouffant (1980) found that the average ratio of chrysotile fiber concentrations found in the lung versus the pleura is 1.8 while for amosite the ratio is 34. This indicates that chrysotile migrates from the lung to the pleura more rapidly than amphiboles resulting in a higher fraction of total fibers in the pleura being composed of chrysotile (3% in the lungs versus 30% in the pleura). With regard to size, the researchers found the size distribution of amosite is virtually identical in the lung and pleura while chrysotile fibers found in the pleura are much shorter than chrysotile fibers found in lung tissue. This suggests that the movement of chrysotile is a result of a combination of translocation and degradation to shorter fibers (or that tissue samples have been contaminated with environmentally ubiquitous short, chrysotile structures). The authors indicate that chrysotile fibers apparently degrade to shorter fibers more rapidly than amosite and translocate to the pleura more rapidly than amosite. Thus, a greater fraction of chrysotile fibers (albeit short fibers) reach the pleura than amosite fibers over fixed time intervals. However, the

results of this study also confirm that the longer amosite fibers do eventually translocate, although on a much more extended time scale than the translocation of chrysotile.

Importantly, the results of this study need to be evaluated carefully. Boutin et al. (1996) showed that the majority of asbestos fibers in the pleura (particularly the long fibers) are aggregated in localized "black spots" (which surround the sites of lymphatic drainage). Thus, if the tissue samples analyzed by Le Bouffant (1980) do not contain representative sets of such spots, the conclusions drawn by Le Bouffant (1980) may be subject to question.

In summation, human pathology studies tend generally to support the findings of other studies regarding the size effects of asbestos (i.e., short fibers tend to clear more rapidly than long fibers, which can be retained in pulmonary tissues for extended periods). They also appear to highlight drastically different behavior between chrysotile and the amphibole asbestos types (particularly tremolite) regarding the heavily favored retention of the latter, which has also been indicated in animal studies. Unfortunately, the ability to draw quantitative conclusions from human pathology studies is hampered by the severe limitations of these studies (Section 5.2).

6.2.4 Studies of Dissolution/BioDurability

Although asbestos minerals are relatively insoluble *in vivo* in comparison, for example, to various fibrous glasses or other man-made mineral fibers (see, for example, Hesterberg et al. 1998a or Eastes and Hadley 1996), they do eventually dissolve in the body. Therefore, this pathway may contribute importantly to the overall biological clearance of asbestos. Moreover, it has been suggested by several researchers (see, for example, McDonald 1998a and other references cited below) that differences in biodurability between chrysotile and the amphiboles may at least partially explain the disparate potencies observed for these fiber types toward the induction of mesothelioma and, potentially, lung cancer (see Sections 7.2.4.2 and 7.3.3.2).

Note that the term "biodurability" is used here to indicate the persistence of a particle or fiber attributable specifically to solubility (in the absence of other clearance or degradation mechanisms). In contrast, the term "biopersistence" is used to indicate the overall persistence of a particle or fiber in the body attributable to the combined effect of all mechanisms by which it might be removed. Thus, for example, while biopersistence can be evaluated *in vivo*, biodurability can best be inferred from *in vitro* dissolution studies so that effects from other clearance mechanisms can be eliminated.

Several studies further indicate that both the *in vivo* biopersistence and the bio-activity (including carcinogenicity) of various fiber types may be linked to their observed, *in vitro* dissolution rates (Bernstein et al. 1996; Eastes and Hadley 1995, 1996; Hesterberg et al. 1998a, 1998b). Such studies, however, typically involve fiber types with dissolution rates that are rapid relative to the rates of clearance by other mechanisms (Sections 6.2.1.1 and 6.2.1.2). In such studies, moreover, the various types of asbestos are typically employed as negative (insoluble) controls. In fact, most of these studies are based on experiments with rats and the 2-year lifetime of a rat is comparable to the anticipated lifetime of chrysotile asbestos in the body and short compared to the anticipated lifetimes for the amphiboles (see below). Therefore, such studies are not particularly sensitive to differences in the relative biodurability of the different asbestos

types. In fact, in the majority of these studies, the dissolution rates reported for asbestos were derived indirectly by analogy with other minerals or are quoted from other studies that derive rates similarly and may therefore be somewhat unreliable. Nevertheless, a review of a subset of these studies is instructive.

Eastes and Hadley (1995 and 1996) report a simple model that reasonably predicts the relative fibrogenicity and tumorigenicity for a range of synthetic fibers based on the dissolution rates of the fibers measured *in vitro*. The authors found that they could explain observations by assuming that the effects of the various fibers are a function of an adjusted dose that accounts for biodurability. Thus,

$$F=f(ax)$$

where "F" is the observed incidence of the endpoint, "f" is the dose-response function proposed for the effect, "x" is the measured dose, and "a" is an adjustment factor that accounts for durability.

In the model, "a" is determined simply as " t_d/t_L " where t_d is the time that a fiber of diameter, "D" remains in the lung and t_L is the lifetime of the exposed animal (e.g., 2 years for rats). This simple model reasonably reconciles the results observed in animal inhalation and injection studies of MMVF's, RCF's, and asbestos for endpoints including lung tumors, degree of fibrosis, and (for intrapleural injection studies) mesothelioma. Based on a chi-square test, the simple model is shown to adequately fit the data to a number of databases reviewed. In contrast, the unadjusted doses do not. Importantly, the dissolution rates used for the various asbestos minerals in this study were estimated by analogy with similar minerals and therefore may be unreliable.

In studies comparing *in vivo* biopersistence with dissolution rates measured *in vitro*, Bernstein et al. (1996) and Hesterberg et al. (1998a), indicate that it is necessary to consider only long fibers (typically longer than 20 μm), because shorter structures are typically cleared by other mechanisms. They also indicate, at least for this type of study in which whole lungs were homogenized and dissolved prior to preparation for asbestos analysis,² that clearance is initially rapid. This reflects muco-ciliary clearance from the upper respiratory tract. Therefore, it is clearance of long fibers from a longer term pool that tracts *in vitro* dissolution rates.

These authors also report that long, soluble fibers (longer than 20 μm) are actually cleared more rapidly than short fibers in these studies. They indicate that this is likely due to long fibers being too long to be effectively phagocytized by macrophages so that they are left to dissolve in the extracellular fluid at neutral pH. Shorter fibers are effectively taken up by macrophages so that dissolution is hindered by the more acidic environment of the phagosomes (pH 4.5) and by the limited volume of fluid within which to dissolve.

²When whole lungs are homogenized to determine lung burden, this includes the largest airways, which initially contain substantial concentrations of material that is rapidly cleared by the muco-ciliary escalator. However, because this material dominates the quantity of material observed, such studies are not useful for tracking the longer term clearance processes that occur in the deep lung.

Law et al. (1991) studied the dissolution of a range of fibers in solutions used as common fixatives for biological samples. The authors report that chrysotile and crocidolite, as well as many other fibers, dissolve at measureable rates in the fixatives studied (Karnovsky's fixative and formalin fixative). They therefore recommend that fiber concentrations and size distributions obtained from tissue samples stored in such fixatives should be evaluated carefully to account for the possible effects of the fixatives.

Although Coin et al. (1994) reported seeing no effective reduction in long fiber ($>16 \mu\text{m}$) chrysotile (nor other evidence of dissolution) in their study of fiber biopersistence, the limited time frame of this study (30 days) may have been too short to allow detectable changes to accumulate.

The most consistent data for the comparative biodurability of chrysotile and the amphiboles (specifically crocidolite) is found in two *in vitro* studies of the dissolution rates of fibers that were conducted under comparable conditions. In the first of these studies, Hume and Rimstidt (1992) measured the dissolution rate for chrysotile asbestos at neutral pH under conditions analogous to biological systems. The dissolution rate that they report for chrysotile converts to: $K_{\text{diss}} = 12.7 \text{ ng/cm}^2\text{-hour}$ and this is reportedly independent of pH. In a comparable study Zoitus et al. (1997) report the following dissolution rate for crocidolite: $K_{\text{diss}} = 0.3 \text{ ng/cm}^2\text{-hour}$, which is 40 times slower than for chrysotile. Dissolution rates for several MMVF's and RCF-1 are also reported in the latter paper, which are listed from fastest dissolving to slowest in Table 6-4.

Table 6-4. Measured *in vitro* Dissolution Rates for Various Fibers^a

Fiber Type	K_{diss} (ng/cm ² -hr)
MMVF 10	259
MMVF 11	142
MMVF 22	119
MMVF 21	23
Chrysotile	12.7 ^b
RCF 1	8
Crocidolite	0.3

^aSource: Zoitus et al. (1997)

^bSource: Hume and Rimstidt (1992)

Note that dissolution rates for other amphiboles, such as amosite are probably no more than a factor of two or three different than that reported above for crocidolite (see, for example, Hesterberg et al. 1998a,b).

To compare the effect of biodurability on the *in vivo* biopersistence of asbestos and other fiber types, both the detailed kinetics of dissolution and the distribution of fiber sizes must be considered.

As reported by Zoitus et al. (1997), at a sufficiently high rate of fluid flow, the rate of mass loss from a fiber is proportional to its surface area, A. Thus:

$$\frac{dM}{dt} = -kA. \quad (\text{Eq. 6-4})$$

This means that for a uniform mass fiber dissolving congruently:

$$1 - \left(\frac{M}{M_0}\right)^{0.5} = 2kt/D_0\rho. \quad (\text{Eq. 6-5})$$

where:

- M is the mass at time t ;
- M_0 is the initial mass at time $t=0$;
- D_0 is the initial diameter of the fiber; and
- ρ is the density of the fiber.

Substituting the equation relating the mass and the diameter of a fiber ($M=\rho\pi d^2 h/4$) into the above equation, cancelling terms, and rearranging indicates that (during dissolution) the diameter of a fiber decreases linearly with time:

$$D = D_0 - 2kt/\rho. \quad (\text{Eq. 6-6})$$

where:

- D is the diameter at time t ; and
- all other terms have been previously defined.

Furthermore, the rate of reduction in radius is given by: k/ρ . Based on the dissolution rates given above for chrysotile and crocidolite, the radius reduction rates (v_{rad}) for these fiber types are determined to be: $1.26 \times 10^{-8} \mu\text{m/sec}$ and $2.6 \times 10^{-10} \mu\text{m/sec}$, respectively. Thus, the dissolution of each fiber is a zero order process (i.e., the rate is constant with time and independent of concentration). Given these rates, a chrysotile fiber $1 \mu\text{m}$ in diameter will disappear in approximately a year ($3.9 \times 10^7 \text{ sec}$) and a crocidolite fiber of the same diameter in approximately 60 years ($1.9 \times 10^9 \text{ sec}$).

The number rate of disappearance of a population of fibers due to dissolution is a function of the rate of radial reduction for the fiber type and the distribution of fiber diameters in the population. The time at which the entire population finally dissolves can be estimated simply by dividing the radius of the largest fiber by the radius reduction rate, v_{rad} , that is appropriate for the fiber type. The number of fibers remaining from the population at time t will be equal to the number of fibers in the original distribution with radii larger than $v_{rad}t$ for the reduction rate that is appropriate for the fiber type.

Note that dissolution will not cause an immediate reduction in fiber concentration. The number of fibers will not begin to decrease until sufficient time has elapsed for the thinnest fibers to completely dissolve. Eastes and Hadley (1994) therefore recommend tracking the time dependence of the mode of the distribution of fiber diameters to best gauge the effects of dissolution *in vivo*.

Importantly, fibers *in vivo* will only dissolve at the rates predicted by the above equations if the fluid in which they are dissolving flows past the fibers sufficiently rapidly to prevent saturation from limiting the rate (Mattson 1994). Especially for slow dissolving materials of limited solubility like asbestos, it is expected that the observed dissolution rate *in vivo* will generally be slower than the rates predicted based on *in vitro* measurements. Even for more rapidly dissolving fibers like most fibrous glasses and manmade mineral fibers, dissolution is hindered in compartments of the body in which the volume of available solute is limited.

In summary, dissolution is a zero-order (i.e., constant with time, independent of concentration) clearance mechanism that is dependent on fiber mineralogy, that the effect it has on fiber populations (concentrations) is a function of the distribution of fiber diameters within the population, and that the theoretical rate of dissolution may not be achieved in all tissues in all compartments of the lung or mesothelium due to limits in the rate of *in vivo* solute flow.

6.2.5 Dynamic Models

Unlike particle deposition in the lungs, which is an entirely mechanical process, clearance, transport, and degradation mechanisms tend to be complex biochemical processes. Due to the incomplete understanding of such processes, state-of-the-art modeling of degradation and clearance is not as advanced as that for deposition. Even the most sophisticated of degradation and clearance models remain semi-empirical. Although, current models in this area show general agreement with the sparse, available data, there are clearly areas of weakness that require additional research. Nevertheless, the models provide a good indication of the kinds of processes that are important in the body and their overall constraints. It is also noted that models for degradation and clearance in humans tend to be better developed than those for animals, primarily due to confounding uncertainties associated with animal ventilation rates. An overview of the state of the art, which was current as of the date of publication, can be found in Stober et al. (1993).

According to Stober et al. (1993), the general conclusions that can be drawn from the current models are that:

- clearance from ciliated airways is rapid, independent of particle/fiber type, apparently independent of particle size, and can be described as the sum of two, weighted exponentials (i.e., an assumed combination of two first-order decay processes), although the process may in fact be zero order (i.e., the reduction in concentration with time is constant and independent of concentration) with rates that differ primarily by the distance that a particle must traverse to return to the trachea.

Based on studies of particle clearance reported by Raabe (1984), muco-ciliary transport in the nose and throat generally exhibits a half-life for clearance of 4 minutes. Clearance of the tracheo-bronchial section of the respiratory tract is a function of the distance from the trachea and generally varies from a half-life of 30 minutes for the largest bronchi to approximately 5 hours for the smallest and most remote bronchi. In healthy humans, material deposited in this region is generally cleared within 24 hours. In contrast, the clearance mechanisms operating in the deep lung, beyond the muco-ciliary escalator, operate over time frames of many days to years (see Table 6-2);

- clearance of insoluble particles from the pulmonary portion of the lung occurs primarily by macrophage transport and such transport has several components. One component represents the population of "free" macrophages located within the alveoli that engulf particles and transports them to the muco-ciliary escalator. Macrophages are also renewed at some rate of recruitment that may be dependent on particle concentrations. In fact, numerous studies have demonstrated that macrophage recruitment is induced by the deposition of asbestos and other particles in the lung (Section 6.3.5). Particles also migrate into the interstitium where another population of macrophages clears these particles to lymph. This second component (interstitial clearance) is much slower than the first (see Table 6-2);
- each macrophage can carry a maximum load and the mobility of each macrophage decreases with increasing load. At sufficient loading, macrophages become immobile and aggregates of overloaded macrophages in the alveoli may then sequester particles for some period of time as this clearance mechanism is shut down. In the interstitium, masses of immobile macrophages may trigger development of granulomas that sequester particles for extended periods of time by effectively preventing clearance of the particles within such tissue, at least until or unless the granulomas resolve. Thus, these models incorporate overload mechanisms and the incorporation of such overload mechanisms are required to explain observed trends in experimental results; and
- in various published studies, overload (immobilization of laden macrophages) has been modeled as dependent on the total volume or mass of phagocytized material (for compact particles) and (additionally) on the length of phagocytized material (for fibers). It is also possible that the motility of macrophages and the consequent overall rate of this clearance process is additionally a function of fiber diameter and/or particle toxicity (the latter for special cases).

Interestingly, while it is reported that large, spherical particles are not readily cleared by this mechanism, the range of sizes over which clearance becomes hindered corresponds reasonably well to the limits of overall respirability. In contrast, fibers that are clearly too long to be cleared by macrophages, if they are sufficiently thin, are quite respirable. Thus fibrous materials present a unique challenge to the respiratory tract based solely on the dimensions of these materials.

Stober et al. (1993) also notes that many models incorporate the assumption that most clearance processes are first order (i.e., that the rate of reduction of mass or fiber number is proportional to the remaining mass or fiber number, respectively, and independent of other factors). Thus, the combined effects of multiple clearance processes can be expressed as a weighted sum of exponentials and this approach has been fairly successful at mimicking actual processes. This means, however, that the half-lives "t_{1/2} 's" attributed to the various first order decays are empirical and do not necessarily correspond to any specific physiological or biochemical features of the processes being modeled. Depending on the specific process, clearance rates may be zero order or may be a more complicated function of multiple variables than can be described by a first order decay. Nevertheless, models incorporating these simplifying assumptions have shown good success at adequately describing observed effects.

Note that half-lives for first order decay processes represent the time required for half of the initial mass to decay (or be transported or whatever) and can be estimated as: t_{1/2}=(ln2)/k with k being the first order rate coefficient or proportionality constant between rate and mass. This is why so many of the retention studies cited above provide estimates of a series of decay constants or half-lives that are assumed to correspond approximately to the major clearance processes contributing to the observed, overall reduction in concentration.

Due to the complexity of the processes involved, only a small number of dynamic models for fiber retention have been developed. Interpretation of the results of these models requires that the meaning of the term "retention" first be reconciled across studies.

Dement and Harris (1979) report that, based on a mathematical model, the fraction of structures retained in the deep lung is unlikely to vary by more than a factor of 2 for different asbestos mineral types. In this study, however, the term retention appears to refer primarily to a very short time period that primarily includes consideration of deposition, but not clearance processes.

Using a definition for retention that reflects long-term residence in the lung, Yu et al. (1990) developed a model of chrysotile retention that explicitly incorporates longitudinal splitting, dissolution, and size-dependent clearance. Time-dependent lung burden estimates derived using the model were shown to compare reasonably well with published data (Abraham et al. 1988, as cited by Yu et al. 1990) both in terms of fiber concentrations and fiber size-distributions.

In a later modification of their retention model for chrysotile, Yu et al. (1991) also considered the effect of airway asymmetry on fiber retention. In this version of the model, Yu and coworkers incorporated information concerning the geometry of the bronchio-alveolar tree (including mean distance and the mean number of airway bifurcations between the trachea and the alveoli in each section of the lung) and studied the effects of such considerations. The modified model predicts a non-uniform distribution of the asbestos that is retained in the lung and the predictions reasonably reproduce the distributions observed by various researchers and measured formally by Pinkerton et al. (as cited by Yu et al. 1991).

Yu and Asgharian (1990) also modeled the long-term retention of amosite in rat lungs. In contrast to the models employed for chrysotile, the model presented for amosite incorporates a term for the clearance rate that is not a constant but, rather, is a function of the lung concentration of asbestos, which was adapted from an earlier model for diesel soot. This

modification was incorporated to adequately mimic the suppression of clearance with increasing lung burden that has been observed by several research groups (e.g., Davis et al. 1978; Wagner et al. 1974) for amphiboles. Conditions under which elevated asbestos (or dust) concentrations are observed to reduce clearance are referred to as "overload" conditions. Model predictions were shown to reasonably reproduce the time-dependence of amosite lung burdens (in terms of mass) in several studies.

Importantly, the overload conditions addressed in the Yu and Asgharian (1990) model were primarily observed among older retention studies where lung burden was tracked as total asbestos mass (Section 6.2.1). Such studies tend to suggest a difference in the behavior of chrysotile and the amphiboles. As indicated in Section 6.2.1, however, later retention studies, which track lung burden as a function of fiber number (in specific size categories) tend to show this effect is a function of fiber length more than fiber type and newer models may need to incorporate such factors that indicate reduced macrophage motility as a function of fiber length.

Moreover, it is important to consider the major, confounding effects, if the goal is to develop a model that not only reproduces the time-dependence of clearance, but also captures relevant physical phenomena. Thus, for example, Yu et al. (1994) were able to reproduce the time-dependence of the retention in rats of inhaled RCF-1 (as a function of fiber size) using a model in which macrophage motility was limited only by total lung burden and not dependent on fiber size. However, these authors also failed to consider that long RCF-1 fibers in fact dissolve at rates competitive with the clearance of short fibers (see Section 6.2.1), which is probably why they did not find a dependence on length; the two effects cancelled out.

6.2.6 General Conclusions Regarding Deposition, Translocation, and Clearance

The current literature on deposition, translocation, and clearance paint a consistent picture of the fate of fibrous structures in the lung. The ultimate fate of biodurable fibers depends overwhelmingly on their size. Although there may be additional effects due to mineralogy (addressed further in Section 6.3) and for rare, special cases this may be important, generally such effects appear to be minor.

The primary effect attributable to mineralogy that is important to consider in relation to clearance is that associated with biodurability. Fibers that dissolve in the lung at rates that are competitive with the other clearance mechanisms described below may be cleared sufficiently rapidly to preclude adverse effects, even when such fibers are too long to be cleared efficiently by macrophages (see Section 6.2.1).

A schematic representation of the complex set of mechanisms that contribute to the translocation and clearance of fibrous structures that have been deposited in the deep lung is presented in Figure 6-4. This description was developed based on the complete spectrum of observations reported in each of the previous sections of this chapter including, primarily, the descriptions of the most sophisticated of the models reviewed by Stober et al. (1993).

FIGURE 6-4:
PUTATIVE MECHANISMS FOR CLEARANCE AND TRANSLOCATION

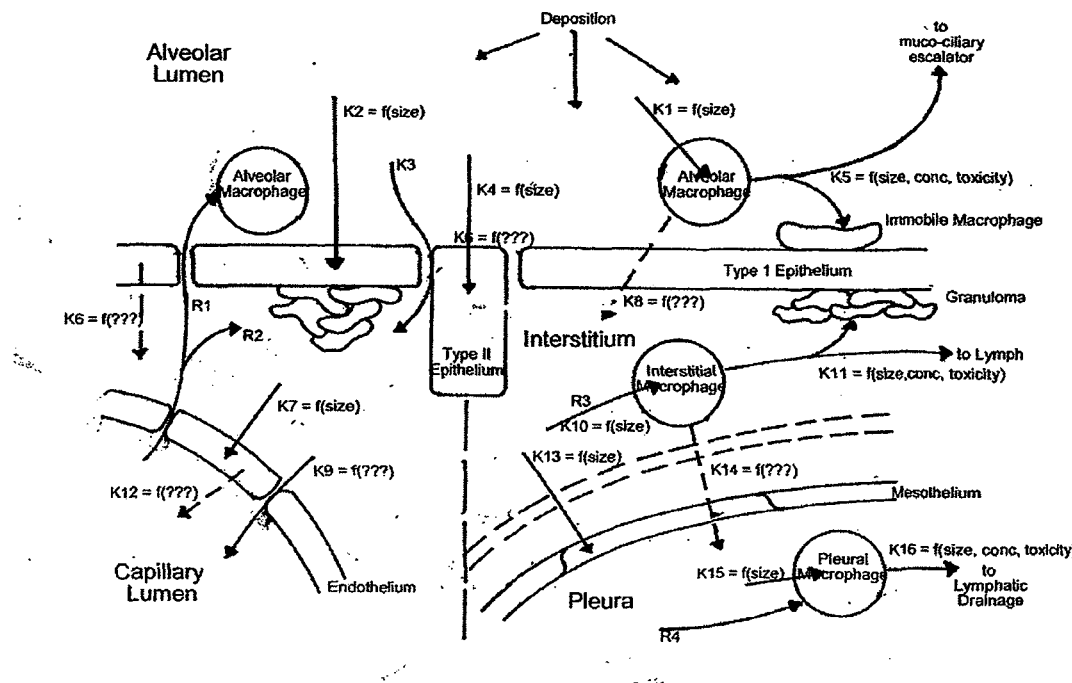


Figure 6-4. Key for Putative Mechanisms for Clearance and Translocation of Fibers in the Lung

- K₁ = rate constant for phagocytosis of fibers by alveolar macrophages. This mechanism is an inverse function of fiber length and, likely, diameter. This mechanism is likely pseudo first order (assuming sufficient numbers of macrophages, the rate will be proportional to the number of fibers);
- K₂ = rate constant for phagocytosis of fibers by Type I epithelial cells. This mechanism is an inverse function of fiber length and, likely, diameter. This mechanism is likely pseudo first order;
- K₃ = rate constant for diffusion of fibers from the alveolar air space (lumen) through the epithelial lining to the underlying interstitium. This mechanism is diffusion limited and likely independent fiber size or type. This mechanism likely parallels the behavior of diffusion in through a finite, column of fixed diameter.
- K₄ = rate constant for phagocytosis of fibers by Type II epithelial cells. This mechanism is an inverse function of fiber length and, likely, diameter. This mechanism is likely pseudo first order;

Figure 6-4 Key for Putative Mechanisms for Clearance and Translocation of Fibers in the Lung (*continued*)

K_5 = rate constant for transport by macrophage to the muco-ciliary escalator. This mechanism is likely an inverse function of fiber length and the volume (or mass) of the fibers phagocytized. Macrophages that become immobilized tend to aggregate in alveolar lumena. For macrophages with fixed loads, this mechanism may be first order or zero order.

K_6 = rate constant for putative discharge to interstitium of phagocytized fibers by Type I epithelial cells. There has been no direct verification of this mechanism;

K_7 = rate constant for phagocytosis of fibers by endothelium. This mechanism is an inverse function of fiber length and, likely, diameter. This mechanism is likely pseudo first order;

K_8 = rate constant for putative mechanism in which fibers internalized by macrophages are transported through the epithelial lining of the alveolar space to the underlying interstitium. There has been no direct verification of this mechanism;

K_9 = rate constant for diffusion of fibers from the interstitium through the endothelial lining to the enclosed, capillary lumen. This mechanism is diffusion limited and likely independent fiber size or type. There has been no independent verification of this mechanism;

K_{10} = rate constant for phagocytosis of fibers by interstitial macrophages. This mechanism is an inverse function of fiber length and, likely, diameter. This mechanism is likely pseudo first order (assuming sufficient numbers of macrophages, the rate will be proportional to the number of fibers);

K_{11} = rate constant for transport by macrophage from the interstitium to the lymphatic system. This mechanism is likely an inverse function of fiber length and the volume (or mass) of the fibers phagocytized. Macrophages that become immobilized tend to induce formation of interstitial granuloma. For macrophages with fixed loads, this mechanism may be first order or zero order.

K_{12} = rate constant for putative discharge to capillary lumena of phagocytized fibers by endothelial cells. There has been no direct verification of this mechanism;

K_{13} = rate constant for phagocytosis of fibers by mesothelial cells of fibers transported to the mesothelium. This mechanism is an inverse function of fiber length and, likely, diameter. This mechanism is likely pseudo first order;

Figure 6-4 Key for Putative Mechanisms for Clearance and Translocation of Fibers in the Lung (*continued*)

K_{14} = rate constant for putative mechanism in which fibers internalized by macrophages are transported from the interstitium through intervening tissue and the mesothelium to the pleural space. There has been no direct verification of this mechanism;

K_{15} = rate constant for phagocytosis of fibers by pleural macrophages. This mechanism is an inverse function of fiber length and, likely, diameter. This mechanism is likely pseudo first order (assuming sufficient numbers of macrophages, the rate will be proportional to the number of fibers);

K_{16} = rate constant for transport by macrophage to sites of lymphatic drainage (lymphatic ducts) along the pleura. This mechanism is likely an inverse function of fiber length and the volume (or mass) of the fibers phagocytized. For macrophages with fixed loads, this mechanism may be first order or zero order.

Not shown: apparently fibers that are too large to pass through lymphatic ducts attract accumulation of macrophages at sites of lymphatic drainage (Kane and MacDonald 1993).

R_1 = rate constant for the renewal of the alveolar macrophage population. While there is likely a steady state rate for background renewal, given that the average life of an alveolar macrophage is reported to be on the order of 7 days, this rate is also stimulated in response to insult by foreign substances in the lung;

R_2 = rate constant for the renewal of the interstitial macrophage population. While there is likely a steady state rate for background renewal, this rate is also expected to be stimulated in response to insult by foreign substances in the interstitial space;

R_3 = rate constant for the renewal of the pleural macrophage population. While there is likely a steady state rate for background renewal, this rate is also expected to be stimulated in response to insult by foreign substances in the pleura;

As shown in Figure 6-4, briefly, the first reaction to the introduction of fibers (or other particulate matter) into the alveolar lumen is scavenging by alveolar macrophages. It has been reported that the initial uptake by macrophages is a rapid process that is essentially complete within hours after initial deposition. Rates for several of the mechanisms depicted in Figure 6-4 have been estimated in the literature and are summarized in Table 6-2.

The rate of removal (to the muco-ciliary escalator) by alveolar macrophages is then determined by a variety of effects. Macrophage motility is a size dependent-process so that only fibers that are sufficiently compact ($\sim 20 \mu\text{m}$) can be removed from the lung. The rate of removal by this process may also be suppressed both for fibers of intermediate lengths (10–20 μm , which are short enough to be phagocytized, but long enough to suppress macrophage motility) and by the overall mass/volume of particles deposited (and, proportionally, taken up by each macrophage). Note that the dimensions provided are the ones that are apparently appropriate for humans. For rats, the corresponding dimensions may be somewhat smaller.

Likely competing with scavenging by macrophages are (1) phagocytosis by the epithelial cells lining the alveolus and (2) diffusive transport to the interstitium. Both Type I and Type II epithelial cells appear to phagocytize fibers. Although relatively few fibers are observed to be taken up by Type II cells, as previously discussed (Section 6.2.2), one possible explanation for the limited observation of fibers in Type II cells is that uptake of fibers induces terminal differentiation to Type I cells. It is expected that phagocytosis by epithelial cells is a size-dependent process.

Especially when the presence of fibers (or other particulate matter) induces morphological changes in Type II cells that increase the overall permeability of the epithelial lining (Section 6.3.7), fibers can apparently diffuse into the interstitium. This process, potentially supplemented with expulsion of phagocytized fibers by epithelial cells and/or transport of fiber laden macrophages through the epithelial lining, represents the set of putative mechanisms by which fibers may reach the interstitium. It is expected that these processes are somewhat slower than uptake by alveolar macrophages (see Table 6-2).

Therefore, if this latter mechanism is operating at peak efficiency, relatively few fibers may reach the interstitium. Note that diffusive transport is likely independent of fiber length, but may be dependent on fiber width with thinner fibers more rapidly diffusing to the interstitium.

Fibers reaching the interstitium are likely cleared primarily by interstitial macrophages, which phagocytize the fibers and transport them to the lymphatic system. Both the efficiency of phagocytosis and motility of macrophage transport in the interstitium likely depend on fiber size and the total volume/mass of fibers in the same way described above for transport by alveolar macrophages. However, all such mechanisms are substantially slower in the interstitium than in the alveolar lumen (see Table 6-2).

Macrophages that have been immobilized (due to fiber size or volume/mass) in the interstitium tend to aggregate and induce formation of granulomas, which may sequester the fibers in these cells. Although there is less evidence for this, fibers free in the interstitial matrix might also trigger such a process. Such fibers would typically be too large to have been effectively phagocytized by any of the cells of the interstitium.

Fibers may also reach the endothelium and be taken up by endothelial cells lining the capillaries of the deep lung. Because fibers have also been observed in capillary lumena, mechanisms similar to those described for transport through the alveolar epithelium to the interstitium may be operating to transport fibers into capillary lumena. While it is expected that such mechanisms will also show size dependence similar to that previously described, little is known about the details or the rates of such processes.

Also by mechanisms similar to some or all of the putative mechanisms described for translocation of fibers from the alveolar lumen to the interstitium, fibers may reach the pleura. Whether fibers can also reach the pleura via transport in blood or lymph has not been definitively determined. Fibers reaching the pleura may be phagocytized by mesothelial cells or may pass through such cells to the pleural cavity. Fibers reaching the pleural cavity are apparently phagocytized by pleural macrophages (probably showing a similar size or volume/mass effect as described above for similar mechanisms) and are apparently transported to (and deposited at) sites of lymphatic drainage along the pleura. If such fibers are then too large to pass through the lymphatic ducts, they may trigger accumulation of additional macrophages and other inflammatory cells.

Overall, the effects of size appear to be:

- few fibers thicker than approximately 0.7 μm and virtually none thicker than approximately 1.5 μm appear to reach the deep lung. Of these, the longer the fiber, the thinner the fiber. Importantly, the distribution of sizes of structures deposited in the deep lung tend to be much more similar across studies than the distributions in the aerosols originally inhaled. Thus, deposition is a very effective filtering process; and
- short fibers (or compact particles) that are shorter than somewhere between 10 and 20 μm tend to be taken up almost entirely by macrophages and are either cleared via the muco-ciliary escalator, isolated in immobilized macrophages that remain within alveolar lumena, or transported to lymphatics (presumably after first reaching the interstitium). These processes appear to be efficient for the shortest of the fibers in this range (and all shorter fibers) so that no further effects are manifest. In contrast, longer fibers, which are not efficiently cleared or isolated by macrophages either in the alveolar lumen or the interstitium appear to trigger a range of additional responses, some of which appear to lead to disease.

Therefore, based on deposition, translocation, and clearance, it is fibers thinner than approximately 0.7 μm and longer than a minimum of approximately 10 μm (with relative contributions increasing with increasing length up to at least 20 μm) that likely contribute to disease. Modifications to this range of structure sizes due to effects attributable to direct biological responses are addressed further in Section 6.3.

Regarding putative differences in behavior between chrysotile asbestos and amphibole asbestos, such effects are adequately addressed by the unifying discussion provided above. To make sense of such differences, the effects of fiber size must first be explicitly considered. Thus, chrysotile fibers may not be as efficiently deposited in the deep lung to the extent that they are curlier or

occur in thicker bundles than amphibole fibers. The overall load of chrysotile deposited in the deep lung may also be cleared more rapidly than amphiboles to the extent that (1) short, thin fibrils ultimately represent a greater fraction of the total load of chrysotile than the amphiboles and (2) a subset of long chrysotile fibers, not sequestered in an environment with limited fluid flow, may be cleared more rapidly than similarly long amphibole fibers due to contributions from dissolution.

Importantly, the concentrations of asbestos to which humans are exposed are much lower than the concentrations to which animals were exposed in the various literature studies cited. Moreover, as indicated in Section 6.1.2, for virtually any exposure of interest, the resulting (volumetric or surface area) lung burden will be substantially higher in rats than in humans. Therefore, overload conditions or other processes that might impede or alter the clearance mechanisms described above, will never occur in humans without first having affected the results of the animal studies reported. Thus, conclusions concerning size-dependence and related effects (except to the extent that they need to be adjusted for cross-species differences) should remain valid when extrapolated between animals and humans.

6.3 FACTORS GOVERNING CELLULAR AND TISSUE RESPONSE

For inhaled structures that survive degradation and clearance, a series of complex reactions between the structures retained in the lung and surrounding tissue may induce a biological response. Asbestosis (fibrosis), pulmonary carcinomas, or mesotheliomas may result. Mesotheliomas are likely associated with structures that are translocated from the lung to the mesenchyme, although diffusible growth promoters and other chemical signals produced by asbestos exposed cells in lung tissue immediately proximal to the mesothelium may also play a role (see Adamson 1997, as described in Section 6.3.4.1).

That the specific biochemical triggers for asbestos-related diseases have not been definitively delineated as of yet is not surprising. Despite great progress in elucidating candidate mechanisms, the number of candidate mechanisms is large and confounded by “cross-talk” between mechanisms. Moreover, similar toxic endpoints may result from entirely independent mechanisms that exhibit disparate dose-response characteristics but, nevertheless, may be triggered by the same or similar toxins. In such cases, however, the relative contributions from each mechanism to a particular endpoint may vary substantially. Unfortunately, the ability to compare results across studies of different mechanisms is currently limited due to the inability to reconcile the quantitative effects of dose and response across dissimilar studies.

Table 6-5 illustrates the range and complexity of the biological responses triggered by asbestos in lung tissue. The table was developed based on the information gleaned from the studies described in this section. Importantly, not all of the mechanisms listed contribute equally to the toxic endpoints that are attributable to asbestos, but their relative importance has yet to be entirely delineated. The toxic endpoints of potential interest to which each of the listed mechanisms potentially contribute are indicated in bold italics.

Table 6-5. Putative Mechanisms by Which Asbestos May Interact with Lung Tissue to Induce Disease Following Inhalation

Asbestos (<i>in vivo</i>)
Generates reactive oxygen species (ROS) <ul style="list-style-type: none"> ● may affect neighboring cells and tissues
Interacts with macrophages
Interacts with lung epithelium
Asbestos interacts with macrophages
Induces generation and release of reactive oxygen species/reactive nitrogen species (ROS/RNS) <ul style="list-style-type: none"> ● may affect neighboring cells and tissues ● may induce inflammatory response (<i>which may promote cancer</i>) ● may induce fibrogenesis (<i>which may promote cancer</i>) ● induces signaling cascades in macrophages and neighboring tissues <ul style="list-style-type: none"> – mediates apoptosis (<i>which may regulate cancer</i>) – mediates proliferation (<i>which may promote cancer</i>) ● causes genotoxic effects in neighboring tissues <ul style="list-style-type: none"> – <i>may cause cancer initiation</i> – may induce arrest of cell cycle – induces signaling cascades <ul style="list-style-type: none"> • mediates apoptosis (<i>which may regulate cancer</i>) • mediates proliferation (<i>which may promote cancer</i>) ● depletes reserves of antioxidants in macrophages and neighboring tissues <ul style="list-style-type: none"> – may induce cytotoxicity (<i>which may promote cancer, by inducing proliferation</i>) – may increase susceptibility to insult by other toxic agents (<i>which may promote cancer</i>)
Induces release of various cytokines <ul style="list-style-type: none"> ● affects neighboring cells and tissues ● mediates inflammatory response (<i>which may promote cancer</i>) ● mediates fibrogenesis (<i>which may promote cancer</i>) ● induces signaling cascades in macrophages and neighboring tissues

Table 6-5. Putative Mechanisms by Which Asbestos May Interact with Lung Tissue to Induce Disease Following Inhalation (continued)

<ul style="list-style-type: none"> – mediates apoptosis (<i>which may regulate cancer</i>) – mediates proliferation (<i>which may promote cancer</i>) ● mediates proliferation in neighboring tissues (<i>which may promote cancer</i>) <p>Induces signaling cascades and mediates apoptosis in macrophages (<i>which may regulate cancer</i>)</p> <p>At high enough concentrations, promotes cytotoxic cell death (<i>which may promote cancer by inducing proliferation</i>)</p>
Asbestos interacts with Lung Epithelium
<p>Induces release of reactive oxygen species/reactive nitrogen species (ROS/RNS)</p> <ul style="list-style-type: none"> ● may affect neighboring cells and tissues ● may induce inflammatory response (<i>which may promote cancer</i>) ● may induce fibrogenesis (<i>which may promote cancer</i>) ● induces signaling cascades in epithelium and neighboring tissues <ul style="list-style-type: none"> – mediates apoptosis (<i>which may regulate cancer</i>) – mediates proliferation (<i>which may promote cancer</i>) ● causes genotoxic effects in epithelium and neighboring tissues <ul style="list-style-type: none"> – <i>may cause cancer initiation</i> – may induce arrest of cell cycle – induces signaling cascades <ul style="list-style-type: none"> • mediates apoptosis (<i>which may regulate cancer</i>) • mediates proliferation (<i>which may promote cancer</i>) ● depletes reserves of antioxidants in epithelium and neighboring tissues <ul style="list-style-type: none"> – may induce cytotoxicity (<i>which may promote cancer by inducing proliferation</i>) – may increase susceptibility to insult by other toxic agents (<i>which may promote cancer</i>) <p>Induces release of various cytokines</p> <ul style="list-style-type: none"> ● affects neighboring cells and tissues ● mediates inflammatory response (<i>which may promote cancer</i>) ● mediates fibrogenesis (<i>which may promote cancer</i>) ● induces signaling cascades in epithelium and neighboring tissues <ul style="list-style-type: none"> – mediates apoptosis (<i>which may regulate cancer</i>)

Table 6-5. Putative Mechanisms by Which Asbestos May Interact with Lung Tissue to Induce Disease Following Inhalation (continued)

	<ul style="list-style-type: none">– mediates proliferation (<i>which may promote cancer</i>)● mediates proliferation in epithelium and neighboring tissues (<i>which may promote cancer</i>)
Causes genotoxic effects	<ul style="list-style-type: none">● <i>may cause cancer initiation</i>● may induce arrest of cell cycle● induces signaling cascades<ul style="list-style-type: none">– mediates apoptosis (<i>which may regulate cancer</i>)– mediates proliferation (<i>which may promote cancer</i>)
Induces signaling cascades	<ul style="list-style-type: none">● mediates apoptosis (<i>which may regulate cancer</i>)● mediates proliferation (<i>which may promote cancer</i>)
Increases epithelial permeability	<ul style="list-style-type: none">● encourages fibrosis (<i>which may promote cancer</i>)● facilitates translocation
At high enough concentrations, promotes cytotoxic cell death (<i>which may promote cancer by inducing proliferation</i>)	

As indicated previously (Section 6.0), although much has been learned about specific components of the underlying mechanisms by which asbestos causes the above-listed diseases, substantial knowledge gaps remain. Moreover, because of these gaps, multiple candidate effects have been explored as potential contributors to carcinogenicity (or fibrogenicity) and one of the goals of this document is to distinguish among those effects that are likely to contribute to the induction of cancer from those that are less likely or unlikely to contribute (given the current state of knowledge). Accordingly, an overview of recent studies is presented below following a brief description of the current model of the general mechanism for cancer. Note that, due to the availability of several recent reviews (including, for example, Economou et al. 1994; Floyd 1990; Kamp et al. 1992; Kane and MacDonald 1993; Mossman and Churg 1998; Mossman et al. 1996; Oberdorster 1994; Robledo and Mossman 1999), only the most recent primary articles are included in the following review.

Also, as indicated below, many of the biological responses provoked by retained asbestos are in fact dependent on fiber size and type. Therefore, studies that distinguish among effects induced by different size fibers (or fibers and non-fibrous particles) of the same mineralogy and studies that distinguish among effects induced by comparably sized fibers (or non-fibrous particles), but differing mineralogy are highlighted. However, due to the limits with which fibrous materials have tended to be characterized in many of these studies, the database from which to distinguish among the effects of size and mineralogy are limited and conclusions from differing studies must be compared with caution.

A large body of evidence supports the conclusion that it is primarily (if not exclusively) long fibers (those longer than a minimum of 5–10 μm) that contribute to disease (see Sections 6.2.1, 6.2.2, and 6.4). Much evidence also indicates that the potency of long fibers increases with length at least up to a length of approximately 20 μm . Therefore, because short and long fibers are both respirable (for fibers that are sufficiently thin, less than approximately 0.7 μm in diameter), differences in the ultimate response to short and long fibers must be attributable to differences in tissue and cellular responses to the retained fibers in each size range.

At least at a histopathological level, clear differences have been observed in the responses evoked by short and long structures (see Sections 6.2.1 and 6.2.2). It is a goal of this section to determine whether the biochemical triggers that mediate the disparate responses to short and long fibers can also be identified. Unfortunately, while a large body of knowledge has been amassed, definitive conclusions are not yet possible. This is because the specific mechanisms by which asbestos acts have still not been definitively determined, although many candidate mechanisms have been elucidated (see above). However, important inferences can still be gleaned from the available studies.

Evidence for the relationship between fiber diameter and disease is somewhat less clear. Although there appears to be a fairly sharp cutoff in the diameter of fibers that are respirable (see Section 6.1.4), several studies suggest that the most potent fibers are substantially thinner than the sharp cutoff in respirability (see Section 6.4). If these latter observations are valid then, as with length, differences in the ultimate response to thick and thin fibers must be attributable to differences in the tissue and cellular responses elicited by retained fibers of each width. As indicated with length, however, definitive conclusions regarding biochemical triggers and the effect of size on such triggers are not yet possible because the specific triggers that lead to

specific asbestos-related diseases have not been definitively identified. Still, useful inferences can be developed.

6.3.1 The Current Cancer Model

The following description of the current model for cancer is derived from the ideas presented in Moolgavkar et al. 1988, Mossman 1993, and Economou et al. 1994.

In the current model of cancer, normal cells must accumulate specific, multiple mutations before a tumorigenic cell is created that can lead to the development of cancer. Each successive mutation produces an initiated cell (a cell that is transformed from normal cells because it incorporates one or more of the requisite mutations, but that has not yet acquired all of the changes needed to produce cancer). Each initiated cell may then proliferate to generate a population of similarly initiated cells, which increases the probability that other events will lead to further mutation in at least one of these cells. Individual mutations may occur spontaneously or may be induced by exposure to mutagens.

Generally, the minimum, heritable changes required before a normal cell is transformed into a metastatic tumor cell include, but may not be limited to (see, for example, Hei et al. 1997 or Kravchenko et al. 1998):

- escape from terminal differentiation or programmed cell death (especially in response to DNA damage);
- escape from anchorage/neighbor dependent growth inhibition;
- development of self-promoting growth and proliferation; and
- active expression of cytokines needed to promote angiogenesis and allow tissue invasion.

It is not clear whether the mutations associated with these changes need to occur in a particular order, although the first of the above-listed changes would facilitate accumulation of all later changes. It is also unclear which of the above changes contribute to the time dependence of tumor development and this may vary among tumor types. It is likely that only a subset of the required mutations determine the ultimate time development of the associated cancer. For example, once a cell begins self-promoting growth, later mutations (even relatively rare ones) may become incorporated rather quickly. Also, some mutations may be rare or may require intervention by a toxic agent, while other mutations may occur spontaneously and may thus occur frequently, once a sufficient number of initiated precursor cells are generated. This is one of the reasons that models with as few as one or two stages have proven successful at predicting the time course of many types of cancer (see, for example, Moolgavkar et al. 1988).

To produce cancer, the mutations that occur must also be "heritable" meaning that they must be preserved and passed on to daughter cells during mitosis. Thus, it is not only necessary to cause alteration in the DNA of a cell (genetic damage), but the mechanisms by which the cell subsequently repairs such changes or prevents cell division (e.g., arrest of the cell cycle, programmed cell death, terminal differentiation) in the presence of such changes must also be defeated. Generally, if a cell proceeds through DNA synthesis (in preparation for mitosis) before accumulated alterations to DNA are repaired, the sites of such alterations can lead to errors in replication during synthesis, which in turn result in permanent, heritable mutations in one or both of the daughter cells that are created from mitosis.

Toxic agents that (directly or indirectly) cause DNA alterations may contribute to the development of cancer by inducing one or more of the set of requisite mutations required for cancer to develop. In traditional parlance, such agents are termed "initiators". In addition, any toxic agent that enhances proliferation also facilitates the development of cancer both by increasing the probability of creating spontaneous mutations (due to errors that infrequently, but unavoidably, occur whenever DNA is synthesized in support of mitosis) and by increasing the numbers of any initiated cells that may be present, which may then serve as additional targets for initiators or may incorporate additional spontaneous mutations. Agents that facilitate the development of cancer by inducing proliferation are traditionally termed "promoters."

Multiple mechanisms have been identified by which both initiators and promoters may act. Initiators, for example, may react directly with DNA to cause genetic damage, or may induce generation of other reactive species (such as reactive oxygen species or reactive nitrogen species) that, in turn, react with DNA to cause genetic damage. In addition, fibrous materials may uniquely damage chromosomes by interfering with mitosis causing aneuploidy (incorporation of an incorrect number of chromosome copies in cells) and/or various clastogenic changes (alterations in the organization and structure of specific chromosomes).

Promoters may also induce proliferation via a variety of mechanisms. Cytotoxic agents, for example, may induce proliferation in a tissue by damaging or killing cells and thereby induce stem cells to proliferate to replace the damaged cells. Promoters may also induce release of various growth factors that, in turn, induce proliferation in targeted tissues. This may occur, for example, as part of the inflammatory response to tissue insult.

Promoters that are biopersistent (such as long asbestos fibers) or promoters that are continually reintroduced (through chronic, external exposure) may also chronically up regulate (or down regulate) certain cell signaling cascades that may contribute to cancer development in a variety of ways including: (1) activation of genes that mediate proliferation or production of various growth factors (including any of various oncogenes) or (2) suppression of genes that inhibit proliferation or growth (including any of various tumor-suppressor genes).

There is growing evidence that all varieties of asbestos fibers (and certain other fibrous materials) can act both as cancer initiators and promoters. However, the biological responses to these materials appear to vary in different tissues so that it may be important to separately evaluate the behavior of asbestos in specific tissues. Biological responses to varying fiber types also appear to vary, particularly in relation to a fiber's biopersistence (Sections 6.2.1 and 6.2.4). Accordingly, an overview of the generic evidence that specific types of asbestos may act as an

initiator and, separately, as a promoter is reviewed below, followed by consideration of the more limited data suggesting tissue-specific variation in biological responses.

6.3.2 Evidence for Transformation

Several recent studies provide evidence that specific types of asbestos can induce transformation of cells in specific tissues (both lung epithelium and mesothelium) to create tumor cells. This provides further, confirmatory support for the whole animal studies in which cancer is induced by exposure to asbestos (see Sections 6.4).

An immortalized, but non-tumorigenic, cell line of human bronchial epithelial cells (BEP2D cells) was transformed by a single exposure to 4 $\mu\text{g}/\text{cm}^2$ UICC chrysotile B (Rhodesian). Surviving cells (the treatment caused 18% cell death) went through several transformations including: altered growth kinetics, resistance to serum induced terminal differentiation, and loss of anchorage dependent growth, before becoming tumorigenic (Hei et al. 1997). Tumorigenicity developed in the various exposed cell lines over a period of several to 11 weeks following exposure. When injected into nude mice, secondary tumors developed with a latency of 8–10 weeks.

The authors indicate that there were no mutations in these cells at either codon 12 or 13 or the ras gene (mutations that have sometimes been observed in asbestos-induced lung cancers. Also, because this cell line already contains alterations in genes for p53 (a protein that plays a role in cell-cycle control, among other things, see Table 6-6) and Rb (Table 6-6), the authors speculate that such changes are not rate controlling for transformation to cancer.

It should also be noted that cultures of Type II cells have been particularly difficult to maintain due to the tendency of these cells to undergo terminal differentiation (to Type I cells) once they are removed from their natural environment in the epithelial lining of lung alveoli (see Leikoff and Driscoll 1993, as described in Section 4.4).

Kravchenko et al. (1998) indicates that, unlike cultures of lung epithelial cells, *in vitro* cultures of rat mesothelial cells tend to transform spontaneously to tumorigenic cells. The major changes that occur with time include: altered response to epithelial growth factor (from growth-proliferation inhibition by this factor to growth-proliferation stimulation), morphological changes (from polygonal epithelial-like cells to elongated fibroblast-like cells and, eventually, polynucleated cells exhibiting broad polymorphism), and multi-layered growth and an ability to grow as colonies and masses in semi-solid agar. Eventually, these cells become immortal and induce cancer when harvested and injected into other rats. The authors indicate that asbestos-induced transformations in such cultures proceed through identical stages, but that they occur much more rapidly. For example, incorporation of the stimulating response to EGF occurs spontaneously at passages 9 or 10, but at passages 6 or 7 when induced by asbestos. Asbestos was applied at 5 $\mu\text{g}/\text{cm}^2$, which was noted to be sub-lethal (95% cell survival was noted at this rate of application).

Table 6-6a. Sources of Various Cytokines and Other Chemical Transmitters

Chemical Species	Abbrev.	Sources	Reference	Effects	Reference
Signal Transmitters					
Activator Protein-1	AP-1			A transcription factor	Mossman and Churg 1998 (Citing: Angel and Karin 1991)
				Binds the DNA promoter region of genes governing inflammation, proliferatin, and apoptosis	
	BAX	Induced by high concentrations of p53	Lechner et al. 1997	Induces apoptosis	Lechner et al. 1997
	Bcl-2			Inhibits apoptosis	Lechner et al. 1997
Fifth Component of Compliment	C5			Mediates asbestos-induced fibrosis	McGavran et al. 1989
Cyclin Dependent Kinases	CDK's			Mediates cell cycle	Lechner et al. 1997
Cyclin Dependent Kinase Inhibitors	CDI's			Inhibits advance of cell cycle	Lechner et al. 1997
	CINC				
Epithelial Growth Factor	EGF			Inhibits proliferation of mesothelial cells	Kravchenko et al. 1998
				Stimulates proliferation of mesothelioma tumor cells	Goodlick et al. 1997
Epithelial Growth Factor Receptor	EGFR			Mediates MAPK signaling	Mossman et al. 1997

Table 6-6a. Sources of Various Cytokines and Other Chemical Transmitters (*continued*)

Chemical Species	Abbrev.	Sources	Reference	Effects	Reference
EGFR regulated kinase	ERK			Mediates apoptosis	Mossman et al. 1997
Granulocyte-macrophage colony Stimulating Factor	GM-CSF				
	GRP78				
Human neutrophil elastase	HNE	Released from asbestos activated PMN	Kamp et al. 1993	By itself, increases pulmonary epithelial cell detachment in culture With asbestos, increases pulmonary epithelial cell lysis	Kamp et al. 1993 Kamp et al. 1993
	HSP72/73				
Intercellular adhesion molecule-1	ICAM-1	Released by lung epithelial and endothelial cells following exposure to silica but not TiO ₂ Enhanced expression by RPM cells exposed to chrys or crc	Nario and Hubbard 1997 Choe et al. 1997	Facilitates migration of leukocytes out of blood to sites of injury	Nario and Hubbard 1997
Interleukin-1	IL-1				
Interleukin-6	IL-6	Induced by ROS in Type II epithelial cells	Luster and Simeonova 1998	Is a pleiotropic cytokine	Luster and Simeonova 1998
Interleukin-8	IL-8			Is a neutrophil chemoattractant	Luster and Simeonova 1998

Table 6-6a. Sources of Various Cytokines and Other Chemical Transmitters (*continued*)

Chemical Species	Abbrev.	Sources	Reference	Effects	Reference
Inducible Nitric Oxid Synthase	iNOS	Expressed by activated macrophages, but not in primates	Jesch et al. 1997		
Keritonizing Growth Factor	KGF	Derived from fibroblasts	Adamson 1997	Induces transient proliferation of mesothelial cells	Adamson 1997
Mitogen Activated Protein Kinase	MAPK			Mediates transcription of AP-1	Mossman et al. 1997
				Mediates ERK signaling	Mossman et al. 1997
Macrophage Inflammatory Protein-1alpha	MIP-1 alpha				
Macrophage Inflammatory Protein-2	MIP-2			A chemoattractant for PMN's, but may not be involved with inflammatory response	Osier et al. 1997
Matrix Metallo-proteinases	MMP's	Relative expression affected by cigaret smoke and fiber exposure	Morimoto et al. 1997		
	Neu				
Nuclear Factor-KB	NF-KB			A transcription factor that regulates genes involved with the inflammatory response, cell adhesion, and growth control.	Barchowsky et al. 1998
Nitric Oxide Synthase	NOS				

Table 6-6a. Sources of Various Cytokines and Other Chemical Transmitters (*continued*)

Chemical Species	Abbrev.	Sources	Reference	Effects	Reference
Ornithine Decarboxylase	odc			Promoted by AP-1 Encodes a key enzyme for the biosynthesis of polyamines	Mossman and Churg 1998
Platelet-Derived Growth Factor	PDGF	Activated macrophages Elevated expression in mesothelioma cells Asbestos and iron treated AM and Interstitial macrophages release PDGF	Bauman et al. 1990 Lechner et al. 1997 Osornio-Vargas et al. 1993	Induces proliferation of lung fibroblasts Induce proliferation of mesothelial cells Is a chemotactic attractant for rat lung fibroblasts	Bauman et al. 1990 Brody et al. 1997 Osornio-Vargas et al. 1993
p53		Induced by DNA damage	Lechner et al. 1997	At low conc, arrests cell cycle at G1/S At higher conc, induces BAX protein, which induces apoptosis	Unfried et al. 1997
Poly(ADP-ribosyl)polymerase	Rb	Inhibited by 3-aminobenzamide	Broaddus et al. 1997		
Tissue inhibitors of MMP's	TIMP's	Relative expression affected by cigaret smoke and fiber exposure			

Table 6-6a. Sources of Various Cytokines and Other Chemical Transmitters (*continued*)

Chemical Species	Abbrev.	Sources	Reference	Effects	Reference
Tumor Necrosis Factor Alpha	TNF-alpha	Some particles induce activated macrophages to release this (shown both <i>in vitro</i> and <i>in vivo</i>)	Driscoll et al. 1997	Induces JNK arm of MAPK cascade	Mossman et al. 1997
		Regulated by oxidant-sensitive transcription of NF-KB	Driscoll et al. 1997	Is involved in the recruitment of inflammatory cells	Driscoll et al. 1997
		Macrophages in BAL from asbestosis and idiopathic interstitial fibrosis patients release TNFalpha	Zhang et al. 1993	Stimulates macrphages, epithelial cells,endothelial cells, fibroblasts to secrete chemokines and adhesion molecules	Driscoll et al. 1997
				Can induce apoptosis among neutrophils	Leigh et al. 1997
				Can induce ROS production in leukocytes	Kaiglova et al. 1999
Transforming Growth Factor Alpha	TGF-alpha			Intradermal inj stimulates local accumulation of fibroblasts and collagen	Zhang et al. 1993
				<i>In vitro</i> , stimulates fibroblast DNA synthesis and proliferation	Zhang et al. 1993
		Expressed in BA epithelium exposed to asbestos	Brody et al. 1997	Is a mitogen for epithelial cells	Brody et al. 1997

Table 6-6a. Sources of Various Cytokines and Other Chemical Transmitters (*continued*)

Chemical Species	Abbrev.	Sources	Reference	Effects	Reference
Transforming Growth Factor Beta	TGF-beta	Expressed in BA epithelium exposed to asbestos	Brody et al. 1997	Inhibits fibroblast proliferation but stimulates formation of extracellular matrix	Brody et al. 1997
		Macrophage stimulated Type II epi cells produce both TGF-beta1 and TGF-beta2	Brody et al. 1997	Can induce apoptosis in different types of cells	Leigh et al. 1997
		All three isoforms expressed in the fibrotic lesions (by hyperplastic type II cells) of asbestos and pleural fibrosis patients from Quebec	Jagiirdir et al. 1997	Does not appear to induce chemotaxis of rat lung fibroblasts	Osornio-Vargas et al. 1993
		Mesothelial tumor cells expressed only TGF-beta1 and 2	Jagiirdir et al. 1997	Induces chemotaxis of rat mononuclear leukocytes	Osornio-Vargas et al. 1993
		Also type II cells of silicosis patients express all three forms	Jagiirdir et al. 1997		
		Asbestos and iron treated AM and Interstitial macrophages release TGF-beta	Osornio-Vargas et al. 1993		
Urokinase-type Plasminogen Activator	uPA			Associated with increased pericellular proteolytic activity in endothelial tissue	Barchowsky et al. 1998

Table 6-6a. Sources of Various Cytokines and Other Chemical Transmitters (*continued*)

Chemical Species	Abbrev.	Sources	Reference	Effects	Reference
Vascular Cell Adhesion Molecule	VCAM-1	Enhanced expression by RPM cells exposed to chrys or crc	Choe et al. 1997		
	WT1			Forms a heterodimer w p53 and alters behavior	Unfried et al. 1997
Enzymes					
Mn-dependent SuperOxide Dismutase	Mn-SOD				
Gene Products					
	c-fos			Linked to apoptosis Transcription factor that activates the TGF-beta1 promotor	Timblin et al. 1998a Jagirdar et al. 1997
	c-jun			Proteins of c-fos dimerize with c-jun to create activator protein-1 (AP-1) Linked to proliferation Transcription factor that activates the TGF-beta1 promotor	Mossman and Churg 1998 Timblin et al. 1998a Jagirdar et al. 1997
	mdm2			Transcription factor that activates the TGF-beta1 promotor	Mossman and Churg 1998
	c-myc			A protococoncogene that inhibits p53	Lechner et al. 1997

Table 6-6b. Effects of Various Cytokines and Other Chemical Transmitters

Chemical Species	Abbrev.	Effects	Reference
Signal Transmitters			
Activator Protein-1	AP-1	A transcription factor Binds the DNA promoter region of genes governing inflammation, proliferatin, and apoptosis	Mossman and Churg 1998 (Citing: Angel and Karin 1991)
	BAX	Induces apoptosis	Lechner et al. 1997
	Bcl-2	Inhibits apoptosis	Lechner et al. 1997
Fifth Component of Compliment	C5	Mediates asbestos-induced fibrosis	McGavran et al. 1989
Cyclin Dependent Kinases	CDK's	Mediates cell cycle	Lechner et al. 1997
Cyclin Dependent Kinase Inhibitors	CDI's	Inhibits advance of cell cycle	Lechner et al. 1997
Cytokine-induced Neutrophil Chemoattractant	CINC		
Epithelial Growth Factor	EGF	Inhibits proliferation of mesothelial cells Stimulates proliferation of mesothelioma tumor cells	Kravchenko et al. 1998 Goodlick et al. 1997
Epithelial Growth Factor Receptor	EGFR	Mediates MAPK signaling	Mossman et al. 1997
EGFR regulated kinase	ERK	Mediates apoptosis	Mossman et al. 1997
Granulocyte-macrophage colony Stimulating Factor	GM-CSF		
	GRP78		
Human neutrophil elastase	HNE	By itself, increases pulmonary epithelial cell detachment in culture	Kamp et al. 1993

Table 6-6b. Effects of Various Cytokines and Other Chemical Transmitters (*continued*)

Chemical Species	Abbrev.	Effects	Reference
	HSP72/73	With asbestos, increases pulmonary epithelial cell lysis	Kamp et al. 1993
Intercellular adhesion molecule-1	ICAM-1	Facilitates migration of leukocytes out of blood to sites of injury	Nario and Hubbard 1997
Interleukin-1	IL-1		
Interleukin-6	IL-6	Is a pleiotropic cytokine	Luster and Simeonova 1998
Interleukin-8	IL-8	Is a neutrophil chemoattractant	Luster and Simeonova 1998
Inducible Nitric Oxid Synthase	iNOS		
Keritonizing Growth Factor	KGF	Induces transient proliferation of mesothelial cells	Adamson 1997
Mitogen Activated Protein Kinase	MAPK	Mediates transcription of AP-1 Mediates ERK signaling	Mossman et al. 1997 Mossman et al. 1997
Macrophage Inflammatory Protein-1alpha	MIP-1 alpha		
Macrophage Inflammatory Protein-2	MIP-2	A chemoattractant for PMN's, but may not be involved with inflammatory response	Osier et al. 1997
Matrix Metalloproteinases	MMP's		
	Neu		
Nuclear Factor-KB	NF-KB	A transcription factor that regulates genes involved with the inflammatory response, cell adhesion, and growth control.	Barchowsky et al. 1998
Nitric Oxide Synthase	NOS		
Ornithine Decarboxylase	odc	Promoted by AP-1	Mossman and Churg 1998

Table 6-6b. Effects of Various Cytokines and Other Chemical Transmitters (*continued*)

Chemical Species	Abbrev.	Effects	Reference
		Encodes a key enzyme for the biosynthesis of polyamines	Mossman and Churg 1998
Platelet-Derived Growth Factor	PDGF	Induces proliferation of lung fibroblasts Induces proliferation of mesothelial cells Is a chemotactic attractant for rat lung fibroblasts	Bauman et al. 1990 Brody et al. 1997 Osornio-Vargas et al. 1993
	p53	At low concentration, arrests cell cycle at G1/S At higher concentration, induces BAX protein, which induces apoptosis	Unfried et al. 1997
Poly(ADP-ribosyl)polymerase			
Tissue inhibitors of MMP's	TIMP's		
Tumor Necrosis Factor Alpha	TNF-alpha	Induces JNK arm of MAPK cascade Is involved in the recruitment of inflammatory cells Stimulates macrophages, epithelial cells, endothelial cells, fibroblasts to secrete chemokines and adhesion molecules Can induce apoptosis among neutrophils Can induce ROS production in leukocytes Intradermal inj stimulates focal accumulation of fibroblasts and collagen <i>In vitro</i> , stimulates fibroblast DNA synthesis and proliferation	Mossman et al. 1997 Driscoll et al. 1997 Driscoll et al. 1997 Leigh et al. 1997 Kaiglova et al. 1999 Zhang et al. 1993 Zhang et al. 1993
Transforming Growth Factor Alpha	TGF-alpha	Is a mitogen for epithelial cells	Brody et al. 1997
Transforming Growth Factor Beta	TGF-Beta	Inhibits fibroblast proliferation but stimulates formation of extracellular matrix	Brody et al. 1997

Table 6-6b. Effects of Various Cytokines and Other Chemical Transmitters (*continued*)

Chemical Species	Abbrev.	Effects	Reference
		Can induce apoptosis in different types of cells	Leigh et al. 1997
		Does not appear to induce chemotaxis of rat lung fibroblasts	Osornio-Vargas et al. 1993
		Induces chemotaxis of rat mononuclear leukocytes	Osornio-Vargas et al. 1993
Urokinase-type Plasminogen Activator	uPA	Associated with increased pericellular proteolytic activity in endothelial tissue	Barchowsky et al. 1998
Vascular Cell Adhesion Molecule	VCAM-1		
	WT1	Forms a heterodimer w p53 and alters behavior	Unfried et al. 1997
Enzymes			
Mn-dependent SuperOxide Dismutase	Mn-SOD		
Gene Products			
	c-fos	Linked to apoptosis	Timblin et al. 1998a
		Transcription factor that activates the TGF-beta1 promotor	Jagirdar et al. 1997
		Proteins of c-fos dimerize with c-jun to create activator protein-1 (AP-1)	Mossman and Churg 1998
	c-jun	Linked to proliferation	Timblin et al. 1998a
		Transcription factor that activates the TGF-beta1 promotor	Jagirdar et al. 1997
		Transcription factor that activates the TGF-beta1 promotor	Mossman and Churg 1998
	mdm2	A protooncogene that inhibits p53	Lechner et al. 1997

Table 6-6b. Effects of Various Cytokines and Other Chemical Transmitters (*continued*)

Chemical Species	Abbrev.	Effects	Reference
c-myc			
H-RAS			
K-RAS			

In a study in which p53 deficient mice were intrapleurally injected with UICC crocidolite (200 µg/week), Marsella et al. (1997) showed that p53 deficient mice exhibited substantially increased susceptibility to development of mesothelioma. In this study, 12.5% of homozygous mice (p53 deficient) developed mesothelioma and the rest died of lymphomas or hemangiosarcomas that develop spontaneously in these mice; 76% of heterozygous mice died of mesothelioma, and only 32% of wild-type mice (p53 competent) died of mesothelioma. The authors suggest that p53 deficient mice are susceptible to excess proliferation induced by crocidolite due to loss of control at the G1/S check point that is normally mediated by p53.

In further confirmation of this hypothesis, Marsella et al. (1997) report in the same study that 7.5 µg/cm² of crocidolite applied to wild murine mesothelial cells in culture induced substantial apoptosis while p53-deficient cells were resistant to apoptosis. The authors also note that most of the p53-deficient cells are tetraploid (suggesting a loss of a spindle check point) while the wild type cells are all diploid.

Note that, although these studies suggest that asbestos alone can induce complete transformation of both lung epithelial cells and mesothelial cells, such studies must be evaluated with caution. In the case of the Hei et al. (1997) study, for example, the effects of the (asbestos-independent) mutations required to initially establish the immortal line of lung epithelial cells are not entirely known. Therefore, the response to asbestos of epithelial cells *in vivo* may be substantially different.

In the case of the Kravchenko et al. (1998) study, it is clear that mesothelial cells *in vitro* do not behave in the same manner as those *in vivo*; *in vitro*, they spontaneously transform to tumorigenic cells. This suggests that one or more growth inhibitory signals exist *in vivo* (which are absent *in vitro*) that are critical to maintaining the health of the mesothelium.

6.3.3 Evidence that Asbestos Acts As a Cancer Initiator

As indicated in a review by Jaurand (1997), historically, the status of asbestos as a mutagen was questioned, due primarily to the failure to produce detectable gene mutations in short-term assays. However, more recent studies provide clear evidence that asbestos (and other fibrous materials) can produce mutations. Moreover, fibrous materials may induce mutations by multiple mechanisms including, for example:

- direct interference with mitosis;
- production and release of reactive oxygen species (ROS); or
- production and release of reactive nitrogen species (RNS).

Of these, the most consistent, positive evidence that asbestos can act as a cancer initiator (i.e., a genotoxin or mutagen) has been from assays designed to detect the kinds of genetic damage that result from interference with mitosis (Jaurand 1997). Although generation of ROS and RNS plays a clear role in mediating asbestos-induced disease, the direct link to a role of asbestos as an initiator is somewhat more tenuous (see Sections 6.3.3.2 and 6.3.3.3).

6.3.3.1 *Interference with mitosis*

Apparently, the physical presence of asbestos fibers can interfere with proper spindle formation and the function of other structural units required for mitosis (Jaurand 1997). This typically leads to aneuploidy (an incorrect number of copies of the chromosomes contained within a cell), development of micronuclei (fragments of chromosomes enclosed in a membrane that are isolated from the main nucleus of the cell), and has also been shown to lead to clastogenic effects (changes in the organization and structure of the

chromosomes). Assays for these kinds of genetic alterations have consistently shown asbestos capable of inducing these effects.

Jaurand (1997) also indicates that:

- fibers must be phagocytized by the target cells before they can interfere with mitosis;
- once phagocytized, all asbestos types are observed to interfere with mitotic activity; and
- samples enriched in long, thin fibers enhance these effects. In contrast, short fibers do not appear to contribute to these effects.

Jaurand (1997) notes, however, that results related to fiber size have not been entirely consistent, primarily because not all studies have rigorously controlled for or even adequately characterized the sizes of the fibrous structures in test materials. Jaurand (1997) also notes that this mechanism is not dependent on the formation of reactive oxygen species or any other reactive free radicals.

Among studies that suggest that surface chemistry (or presumably fiber type) may not be an important factor in determining the degree to which asbestos (or other fibrous materials) interfere with mitosis, Keane et al. (1999), exposed cultured V79 cells (hamster lung fibroblasts) to untreated and HCl-treated chrysotile asbestos. The acid treatment substantially reduces the magnesium content on the surface of the chrysotile. The authors also noted a "small" effect on fiber size due to treatment (treated fibers showed a 20% excess of short fibers). Cells were exposed to doses ranging between 0.4 and 12.7 $\mu\text{g}/\text{cm}^2$ (each dose left in place for 24 hours and then rinsed off). Cells were harvested after an additional 24 hours and evaluated for cytotoxicity and the presence of micronuclei.

Results from the Keane et al. (1999) study indicate that untreated fibers were shown to be slightly more cytotoxic than treated fibers, but both treated and untreated fibers were observed to increase the abundance of micronuclei in a similar, dose-dependent fashion. The induction of micronuclei appeared to saturate at approximately 35/1,000 cells observed at an applied asbestos concentration of 40 $\mu\text{g}/\text{cm}^2$. In contrast, substantial cytotoxicity was only observed at the highest doses employed. The authors thus concluded that surface chemistry (at least in terms of magnesium content) does not appear to have a major affect on induction of micronuclei and that the observed genetic damage and cytotoxicity appear to occur through entirely independent mechanisms.

In other studies, cultured cells were assayed for a variety of genotoxic effects following exposure to a range of fibrous materials.

For example, Dopp and Shiffmann (1998) dosed human amniotic fluid (HAF) cells or Syrian Hamster Embryo (SHE) cells with UICC amosite, Rhodesian chrysotile, crocidolite, or ceramic fibers at concentrations of 0.5, 1.0, 5.0, and 10.0 $\mu\text{g}/\text{cm}^2$ and assayed the cultures for formation of micronuclei and a variety of clastogenic effects.

Based on their study, Dopp and Shiffmann (1998) report that all asbestos types induced formation of micronuclei in SHE cells in a dose-dependent fashion at rates that were significantly elevated over control animals. The effect appeared to saturate at doses between 1 and 5 $\mu\text{g}/\text{cm}^2$ and rates appeared to peak at between 48 and 66 hours post-exposure. Ceramic fibers, which were noted to be longer but thicker than the asbestos fibers tested, also showed significantly increased induction of micronuclei, but at rates less pronounced than for asbestos. However, it is difficult to judge whether this is due to differences in fiber type because the data in the paper are not adequate to distinguish effects of fiber size and number from effects of fiber type. Similar results were obtained with HAF cells, but overall rates were about one third those observed in SHE cells.

The authors also note observing various disturbance of chromatin structure during interphase. They report observing formation of chromatin bridges and chromosome displacements in meta and anaphases and impaired chromatin separation in mitosis. They also report that cytokinesis was frequently blocked.

In addition to the effects that they observed that are attributable to fiber interference with mitosis, Dopp and Shiffmann report observing a variety of clastogenic effects. In all cases where the authors labeled specific regions of specific chromosomes, fiber-exposed cells showed significantly greater frequencies of DNA breaks over controls or gypsum-exposed animals. Different regions of various chromosomes also showed significantly different frequencies of breakage with patterns that were specific to the different fiber types. The authors hypothesize that the observed clastogenic effects may be due to production of reactive oxygen species, to formation of some type of clastogenic factor, or to the direct interactions between fibers and chromosomes during mitosis that are the apparent cause of the disturbances discussed in the previous paragraphs. However, It was not possible to distinguish among hypothetical causes of the observed clastogenic effects in this study.

Kodama et al. (1993) exposed cultures of human bronchiolar epithelial (HBE) cells to asbestos (chrysotile at 0 to 4 $\mu\text{g}/\text{cm}^2$ and crocidolite at 0 to 300 $\mu\text{g}/\text{cm}^2$). They then examined cells at 24, 48, 72, and 96 hours following exposure for cytotoxic effects and cytogenetic effects. Results indicate that both fiber types induced concentration-dependent inhibition of cell proliferation and colony-forming ability, but chrysotile was 100 to 300 times more toxic. The authors report this translates to a 40-fold increase in toxicity on a fiber for fiber basis (although the range of sizes included in this count is not indicated).

Kodama et al. (1993) also report that, at 72 hours, chrysotile (4 $\mu\text{g}/\text{cm}^2$) caused a 2.7-fold increase in binuclei and a 1.6-fold increase in micronuclei. Over the same time interval, at 300 $\mu\text{g}/\text{cm}^2$, crocidolite caused a 1.9-fold increase in binuclei, but did not cause micronuclei. They also report that chrysotile failed to produce significant numerical chromosome changes in HBE cells and increased structural aberrations only at the 24-hour time point. The frequency of neither aneuploidy nor polyploidy was increased at any time point following exposure to asbestos in this study. The authors indicate that this contrasts with observations of relatively high incidences of asbestos-induced chromosome changes observed in some rodent cell cultures and clastogenic effects observed in human mesothelial cell lines. They further speculate that phagocytic cells with high mitogenetic activity are likely most susceptible to the effects of asbestos, which primarily interferes with mitosis. However, they suggest that epithelial cells that are exposed to fibers may undergo terminal differentiation (from Type II to Type I cells) and thus cease mitosis. This would effectively prevent adverse genetic effects from asbestos exposure. Such pathways are not available to mesothelial cells.

Hart et al. (1994) studied the effects of a range of fiber types (with varying size distributions) on Chinese hamster ovary (CHO) cells. The authors indicate that such cells are very different from cells in pulmonary tissues in that they are immortalized, aneuploid, undifferentiated, and preneoplastic. They also note that the responses observed in these cells differs from responses observed in cells from pulmonary tissues. Nevertheless, the implications concerning fiber size are instructive. Fibers evaluated included long, medium, short, and UICC crocidolite and chrysotile along with a range of MMVF's, RCF's, and fibrous glasses. Exposure concentrations ranged between 10 and 225 $\mu\text{g}/\text{cm}^2$.

Results from the Hart et al. (1994) study indicate that all of the fibers caused qualitatively similar toxic effects: concentration-dependent reduction in cell numbers and an increase in the incidence of abnormal nuclei with little or no loss in viability. Fiber-induced cell death in CHO cells appears to be minor, even at relatively high exposure concentrations. Based on mean dimensions (which is problematic), the diameter dependence on the observed toxic effects, particularly on the formation of aberrant nuclei, was slight or absent. However, the effect with length was striking. For lengths up to at least 20 μm , potency toward both cytotoxicity and the induction of aberrant nuclei increased dramatically with increasing length. The authors also note that the lack of an observed fiber composition associated effect on the

toxicity of CHO cells does not correlate with findings from recent rodent inhalation studies using the same test fibers. The authors therefore speculate that CHO cells may not represent an appropriate *in vitro* model for fiber effects. However, it may also be that effects *in vitro* occur over time scales that are rapid relative to those that occur *in vivo* so that biodurability is not important *in vitro*.

In a study by Takeuchi et al. (1999) cultured human mesothelioma cells (MSTO211H) and, separately, cultured human promyelocytic leukemia cells (HL60), which are not phagocytic, were dosed with crocidolite between 0.6 and 6.6 $\mu\text{g}/\text{cm}^2$ (no size range indicated). Studies with latex beads confirmed that the mesothelioma cells are actively phagocytic, but that the leukemia cells are not. The authors indicate that dosed mesothelioma cells showed significantly increased numbers of polynucleated cells, tetraploid cells, and cells with variable DNA content at the G0/G1 transition in the cell cycle and that the extent of effects was dose-dependent. Leukemia cells showed no such effects.

The authors further indicate that, when the mesothelioma cells were sorted by fiber content, those with the highest fiber content showed the greatest effects. The authors also indicate that cells are stimulated neither to release superoxide nor NO at the concentrations of crocidolite studied. However, they hypothesize that intracellular ROS may have been generated because they report finding increased levels of 8-OH-dGua (and oxidized form of one of the DNA bases) following crocidolite exposure. Nevertheless, the authors conclude that the mechanisms by which crocidolite induce cytotoxicity and, potentially, carcinogenicity is related to phagocytosis. Importantly, the effects described in the Takeuchi et al. study are entirely consistent with effects attributable to interference with mitosis, despite any speculation by the authors.

6.3.3.2 Generation of reactive oxygen species (ROS)

ROS have been implicated as mediators in a variety of toxic effects (including cancer initiation) associated with a broad range of toxins (see, for example, Floyd 1990). Moreover, substantial evidence indicates that asbestos can induce generation of ROS by several mechanisms and that asbestos-induced ROS play a role in several of the toxic effects attributable to asbestos (see below). However, whether ROS play an important role in asbestos-associated cancer initiation is less clear and needs to be evaluated carefully. Therefore, evidence that asbestos induces the production of ROS and that ROS contribute to the adverse health affects attributable to asbestos are reviewed below with particular attention to effects that may contribute to the initiation of cancer. Contributions by ROS to other asbestos-related toxic effects are also evaluated in later sections of this chapter.

Note, that generation of certain reactive nitrogen species (specifically the peroxinitrite ion) is closely associated with ROS generation so that evidence for the generation of certain reactive nitrogen species (Section 6.3.3.3) constitutes additional evidence for the generation of ROS.

Asbestos-induced Generation of ROS. Asbestos has been shown capable of generating a variety of reactive oxygen species (ROS) including hydrogen peroxide (H_2O_2), superoxide (O_2^-), and hydroxyl radical (OH^\cdot) via several mechanisms (see, for example, Fubini 1997; Jaurand 1997; Kamp et al. 1992) including:

- catalytic production of superoxide from oxygen in aqueous solution;
- catalytic production hydrogen peroxide from oxygen in aqueous solution;
- catalytic production of hydroxyl radical by the Fenton reaction (degradation of hydrogen peroxide catalyzed by iron on the surface of fibers or mobilized from the surface of fibers);

- catalytic production of several ROS by redox cycling of iron on the surface of fibers or mobilized from the surface of fibers (Haber-Weiss type reactions);
- catalytic production of ROS by release of heme and heme protein from various cellular components;
- by inducing release of various ROS species from phagocytes during “frustrated” phagocytosis; and
- by binding to cell receptors or other features of surface membranes that trigger signaling cascades mediating the production and release of various ROS (and RNS).

For a general review of the chemistry involved in these processes, see Floyd (1990).

Fenton, Haber-Weiss, and Related Reactions. Most of the evidence for Fenton and Haber-Weiss reactions (and related free radical generating reactions) that take place on the surface of asbestos fibers comes from experiments in cell-free systems (see below). Therefore, their relevance to the conditions found *in vivo* may be limited. Moreover, the size of the fibers (especially in terms of their cumulative surface area) and the history of their surfaces (in terms of metal contaminants or coatings that might be present) may substantially alter the effects of such experiments (Fubini 1997). Unfortunately, however, few of the available studies report characterization of fiber sizes or surface conditions in sufficient detail to judge the importance of these effects.

For fibers. Zalma et al. (1987) evaluated a range of fibers (UICC crocidolite, UICC amosite, UICC Canadian and Zimbobwean chrysotile, industrial chrysotile, and magnetite) for their ability to produce free radicals by the direct reduction of oxygen in aqueous solution. In some cases, hydrogen peroxide was also added to the solution. Results indicate that all of the fibers tested were able to generate hydroxyl radicals (even in the absence of hydrogen peroxide), but that the efficiency of production was a strong function of the activation (by grinding) or pacification (by coating with benzene or other agents) of the fiber surface. Chrysotile was reported to be the most efficient at generating radicals and the authors assumed that this is due to iron contamination on the surface (since iron is not a component of the “ideal” chrysotile fiber). However, such conclusions are difficult to evaluate in the absence of simultaneous consideration of fiber size.

Governa et al. (1998) evaluated the ability of wollastonite fibers to generate ROS in both a cell free system and a suspension of polymorphonucleocytes (PMN's). The fibers were observed to produce ROS in both systems and that ground wollastonite produced substantially more ROS than unground. The efficiency of ROS generation in PMN suspension is also reported to be greater for wollastonite than for either chrysotile or crocidolite (tested in previous studies). However, no size information is given. Based on additional work with various inhibitors added to the system, the authors also indicate that only a fraction of the ROS generated was composed of hydroxyl radicals.

Brown et al. (1998) subjected several different fiber types (amosite, silicon carbide whiskers, RCF-1, and various fibrous glasses) to two standard chemical assays for free-radical production (in cell-free systems). The authors indicate that, of the fiber types tested, only amosite showed free radical activity significantly above controls in both assays and only RCF-1 additionally showed significantly elevated free radical activity in one assay. However, there is not enough information provided in this study to determine whether the observed differences are due to differences in fiber sizes, sample preparation (i.e., surface condition), or fiber type. In apparent contrast, for example, Gold et al. (1997) report that amosite and crocidolite produce few free radicals in cell free systems, unless they are ground.

Weitzman and Graceffa (1984) indicate that chrysotile, crocidolite, and amosite are all capable of catalyzing the generation of hydroxyl radicals and superoxide from hydrogen peroxide *in vitro* and that, based on experiments with various iron chelators, these reactions are iron dependent. The authors further indicate that hydrogen peroxide is produced in large quantities as a normal bi-product of tissue metabolism, but that it is effectively scavenged by various enzymes. The authors speculate that, by physically damaging cell membranes, asbestos may allow release of the precursor hydrogen peroxide before it can be scavenged.

For particles. Silica, residual fly ash, and ambient air dusts also can create ROS *in vitro* and the efficiency of production correlates with ionizable concentrations of various transition metals complexed on the dust (Martin et al. 1997). *In vivo*, such metal containing particles also cause release of ROS from macrophages (Martin et al. 1997). Additionally, binding of silica to plasma membranes of airway lung cells and phagosomes provokes generation of ROS.

Castranova et al. (1997) further indicate that it is the concentration of contaminating iron on the surface of freshly fractured quartz that enhances free radical production in aqueous solution (in cell free systems). These authors also showed that high iron-containing (430 ppm) quartz dust inhaled by rats (at 20 mg/m³ for 5 hours/day for 10 days) induced 5 times more leukocyte recruitment, 2 times more lavageable red blood cells, 30–90% increase in macrophage production of ROS, 71% increase in nitric oxide production by macrophages, and 38% increase in lipid peroxidation of lung tissue than observed in rats exposed to low iron-containing (56 ppm) quartz.

Although iron is required for the reactions considered here, studies indicate that the iron content of the fiber itself is not a good indicator of reactivity (Gold et al. 1997). Studies also indicate that the iron that participates in these reactions need not originate with the fiber (Fubini 1997; Jaurand 1997) and biological systems contain abundant sources of iron. Therefore, both iron-containing fibers and iron-free fibers have been shown to participate in these reactions *in vivo*.

Release of heme and heme protein. At least one research group (Rahman et al. 1997) indicates that heme and heme protein cause extensive DNA damage in the presence of asbestos *in vitro* and, based on previous studies, that this may involve heme catalyzed production of ROS following asbestos-induced release of heme from cytochrome P-450, from prostaglandin H synthetase (or perhaps from other heme containing proteins). Importantly, the authors indicate that such observations relate to a nuclear pool of heme, which suggests that ROS generation via this mechanism may occur in the immediate vicinity of DNA. The work by this group suggests at least one additional pathway by which asbestos may induce the production of ROS and by which ROS-mediated damage to DNA might occur.

Frustrated phagocytosis. Numerous studies indicate that long asbestos fibers (longer than somewhere between 10 and 20 µm) cannot be efficiently phagocytized by macrophages (see, for example, Sections 4.4 and 6.2) and that macrophages that are damaged by such “frustrated” phagocytosis release ROS (see, for example, Kamp et al. 1992; Mossman and Marsh 1991). Due to the differences in the size of macrophages across species (see discussion of Krombach et al. [1997] in Section 4.4). The minimum length beyond which phagocytosis may become frustrated may differ in different animals. However, it is clearly longer fibers that contribute to this mechanism for generating ROS. Shorter fibers (<10 µm) are unlikely to cause frustrated phagocytosis in any of the mammalian species of potential interest.

Lim et al. (1997) showed that alveolar macrophages in culture (after stimulation with lippopolysaccharide) generated free radicals (ROS) when subsequently exposed to chrysotile, crocidolite, or amosite (all UICC). They found chrysotile to be the most potent inducer of free radical activity (which is not surprising given that UICC chrysotile contains the highest fraction of long fibers of the UICC samples tested (Berman, unpublished). Based on tests with various inhibitors, the authors indicated that

the free radicals generated by the alveolar macrophages occurred through a pathway mediated by protein tyrosine kinase, phospholipase C, and protein kinase C and that the effects are dose-related.

Kostyuk and Potapovich (1998) cultured peritoneal macrophages and showed that treatment with chrysotile asbestos (1 µg, no size data given) resulted in production of frustrated phagocytosis and cell injury (the latter as evidenced by release of lipid dehydrogenase, LDH, a marker for membrane damage). By working with various chelators and flavonoids (natural plant products, some of which quench superoxide and some of which chelate iron), the authors indicate that cell injury was likely induced by superoxide and that the superoxide was likely produced by an iron-dependent mechanism. Note that this contrasts with the above studies that suggests production of radicals by frustrated phagocytosis in culture is an iron-independent mechanism.

At least for one kind of phagocyte: polymorphonucleocytes (PMN's), a study by Ishizaki et al. (1997) suggests that crocidolite and erionite may induce production of ROS from PMN's by each of two mechanisms. The first requires phagocytosis and may represent the traditional, "frustrated" phagocytosis pathway indicated above. The second pathway is triggered by an interaction between the fiber and the cell surface and is mediated by NADPH. The authors also cite evidence that chrysotile may similarly act through both of these pathways.

Afaq et al. (1998) cultured alveolar macrophages and peripheral red blood cells (RBC's) that were harvested from rats 30-days following a single 5 mg intratracheal instillation of UICC crocidolite, UICC chrysotile, or ultrafine titanium dioxide. The authors indicate that populations of alveolar macrophages were significantly increased (over sham-exposed rats) for all three particle types and that acid phosphatase and lipid dehydrogenase (LDH), which are markers of cell membrane damage, were observed in cell-free lung lavage from animals exposed to all three particle types. Both alveolar macrophages taken from asbestos-exposed animals (both types) showed significantly elevated lipid peroxidation and hydrogen peroxide production over titanium dioxide exposed animals. However, the latter also showed elevated peroxidation and peroxide production that were significantly elevated over sham-exposed animals. Similar results were observed among RBC's from asbestos-exposed animals, but not from titanium dioxide-exposed animals. Note, it is possible that ROS production induced by TiO₂ occurs by a different mechanism (or set of mechanisms) than that for asbestos (see, for example, Palekar et al. 1979, Section 6.3.4.4).

In vivo Evidence for Asbestos-generated ROS. Several studies involving whole animals also indicate that asbestos exposure induces the generation of ROS. Importantly, in such studies, evidence for generation of ROS is generally determined based on observation of the putative effects of ROS, rather than ROS directly.

Ghio et al. (1998) intratracheally instilled 500 µg of crocidolite (NIEHS) into rats. This was observed to induce a neutrophilic inflammatory response within 24 hours (in contrast to saline-exposed rats). The authors collected chloroform extracts from exposed lungs and subjected them to electron spin resonance (ESR) spectrometry. Results indicate the presence of a carbon-centered radical adduct that has a structure consistent with products of lipid-peroxidation. The radical signal was only observed in asbestos-exposed animals and persisted even after one-month following exposure. The authors also report that depletion of neutrophils did not affect the signal and that dextrin-induced inflammation did not produce the signal.

Yamaguchi et al. (1999) studied effects in rat lung tissue at 1, 3, 5, 7, and 9 days following a single intratracheal instillation of 2mg of either glass fiber or UICC crocidolite. The authors indicate significantly increased levels of 8-OH-Guanine (an oxidized form of the DNA base Guanine) one day after crocidolite instillation and increasing repair activity for this oxidized form of guanine with time that became significant at days 7 and 9 following instillation. Glass fibers (noted to be non-fibrogenic and

non-tumorigenic) did not produce either increases in 8-OH-Gua or its repair activity. The effects associated with crocidolite were all noted to be dose related.

Several of these studies also suggest distinctions in ROS generation (either the absolute generation of ROS or generation of specific ROS species by specific tissues) due to differences in fiber (or particle) size or type.

Nehls et al. (1997) intratracheally instilled rats either with quartz (2.5 mg) or corundum (2.5 mg). The latter mineral is reportedly non-tumorigenic. Results indicate that lung epithelial cells in quartz exposed rats exhibited increased 8-oxo-Guanine levels (a DNA adduct generated by reaction with ROS, see above) that persisted for up to 90 days post-exposure. Elevated levels of the DNA adduct appeared in all cell types in all areas of the lung. The authors suggest that the observed persistence of the elevated levels of 8-oxo-Guanine suggests that it was produced at a rate in excess of the lung's capacity for repair. The authors also report enhanced and persistent inflammation, cell proliferation, and an increase in neutrophil population in bronchio-alveolar lavage (BAL) fluid and an increase in tumor necrosis factor alpha (TNF- α) in BAL fluid in the quartz exposed animals. TNF- α is a cytokine linked to a variety of effects including the recruitment of inflammatory cells (see Table 6-6). In contrast, exposure to corundum produced none of the effects observed with quartz.

Timblin et al. (1998b) report that ROS induced responses by rat lung epithelial cells vary depending on whether exposure is to crocidolite, hydrogen peroxide, or cadmium chloride ($CdCl_2$). In response to ROS generation induced by the first two agents increased levels of cJun protein (a protooncogene, Table 6-6) is observed. Further, crocidolite, but not hydrogen peroxide, causes elevation in the levels of manganese-containing superoxide (MnSOD) dismutase (an enzyme that catalyzes dismutation of superoxide, Table 6-6). Neither of these agents affect levels of either of two common stress proteins (Table 6-6): GRP78 or HSP72/73, nor do they affect cellular glutathione levels. In contrast, cadmium chloride does not alter MnSOD levels, but increases levels of GRP78 and HSP72/73 in addition to cJun protein. Therefore, ROS-related mechanisms may be complex and may be toxicant-specific. Thus, it may not be correct to assume that all fibers and particles act through common ROS-related pathways.

In contrast to the results of the above study (which showed no effect on glutathione levels), Golladay et al. (1997) showed that human lung epithelial cells (cultured A549 cells) exposed to crocidolite (NIEHS sample) showed substantial reduction in intracellular levels of glutathione (without increases in the oxidized forms of glutathione). Rather, an associated increase in extracellular, reduced glutathione was observed, suggesting that crocidolite induces release of glutathione from the interior of these cells to the environment. The authors also indicate that, given that the half-life for reduced glutathione outside of cells is on the order of an hour, while extracellular reduced glutathione levels remained elevated for more than 24 hours following exposure, cells must have been releasing reduced glutathione continuously. Because no concomitant release of LDH or labeled adenine was observed (despite loading of cells with labeled adenine prior to the experiment), the authors conclude that release of glutathione is not associated with membrane disruption or apoptosis (which is induced to some degree by exposure to crocidolite). Also, all of the effects described above were similarly associated with exposure to de-ironized crocidolite. Thus, the iron content of the fibers does not play a role in this process.

Note that the apparent difference in the reported effect of crocidolite exposure on intracellular glutathione levels in the above two studies might be due (individually or in combination) to differences in the cell-types studied, differences in the size distribution of the crocidolite employed, differences in study design, or other factors. Insufficient information is available to distinguish among these possibilities.

Kaiglova et al. (1999) intrapleurally injected rats with 10 mg of long amosite and collected bronchio-alveolar lavage (BAL) fluid 24 hours following exposure and at later time intervals. They indicate that total protein and alkaline phosphatase (AP) were both elevated in BAL 24 hours after exposure and that

AP remained elevated for at least 3 months following exposure. They also noted increased levels of lipid peroxides in BAL at 24 hours, but not 3 months following exposure. The authors indicate that antioxidants were significantly decreased following exposure: glutathione was significantly decreased in lung tissue at both 24 hours and 3 months following exposure, but was normal in BAL fluid at all time points; α -tokopherol and retinol were significantly decreased at 3 months in lung tissue; and ascorbic acid was significantly decreased in both lung tissue and BAL at 24 hours and remained low at 3 months. The authors indicate that decreases in antioxidants implies a role for ROS (or RNS) in lung tissue injury. It is also possible that the varied responses of specific antioxidants may suggest a role for toxin- and injury-specific ROS/RNS.

Conclusions Concerning Generation of ROS. Except for frustrated phagocytosis (which is unique to long fibers), ROS generation by the mechanisms discussed above are considered a common response to respiration of particles in general (see, for example, Martin et al. 1997 who suggest that ROS "...may be a global signaling mechanism mediating response to particulate insult mostly by activation of kinases and transcription factors common to many response genes." They further indicate that if the load of ROS generated is too great, or the airway in which it is generated has been previously impaired, "...these same mechanisms can result in deleterious respiratory lesions and outright pathology"). However, not all non-fibrous particles are similarly capable of inducing production of ROS. As indicated above, for example, while crystalline silica is a potent inducer of ROS production, carundum is not (Nehls et al. 1997). Moreover, the spectrum of ROS (set of species) that are induced by particular toxicants are generally specific to the offending toxicant (Timblin et al. 1998b). Therefore, the generic grouping of ROS mediated pathways by particles and, especially, by particles and fibers, does not appear justified. These mechanisms are more complex and individualized than such generic grouping suggests.

ROS can be generated by multiple pathways that are variously dependent on particle size, whether a particle is a fiber, fiber size, and particle or fiber type (i.e., chemical composition). The primary mechanism(s) through which ROS are generated in response to one type of particle or fiber may be very different than that through which ROS generation is induced by another and the resulting suite of ROS (set of species) may also differ. Importantly, the relationship between dose and response for each mechanism may also differ (see, for example, Palekar et al. 1979, Section 6.3.4.4).

Given the above, comparing among the ability of fibrous materials and non-fibrous analogs to induce generation of ROS requires that such analogs be properly matched before valid conclusions can be drawn. Thus, for example, the appropriate non-fibrous analog for crocidolite is the massive habit of reibeckite and the appropriate analog for chrysotile is the massive habit of antigorite or lizardite. Due to differences in both chemistry and crystal structure, crystalline silica is not an appropriate non-fibrous analog for any of the asbestos types. Moreover, because ROS can be generated by different mechanisms, critical comparison across analogs requires more than the simple confirmation that ROS are generated or even whether the relative efficiency with which ROS are generated is comparable. It is also necessary to contrast the specific complexion of ROS (set of species) generated and the specific tissue/cellular environments (i.e., locations within a cell) in which they are generated in response to each analog.

It is also clear that ROS are generated by both iron-dependent and iron-independent pathways. Even for the iron-dependent pathways, however, the source of iron need not derive from the fibers or particles themselves. Therefore, since iron is abundant *in vivo* (and the environment), both iron-containing and iron-free fibers (or particles) can potentially participate in both the iron-independent and the iron-dependent pathways.

Effects Mediated by ROS. ROS have been implicated as mediators in a variety of toxic effects (including cancer initiation) associated with a broad range of toxins (see, for example, Floyd 1990; Martin et al. 1997). Cellular and tissue effects that have been associated with the effects of ROS include:

- enhancement of overall uptake of particles by epithelium;
- stimulation of inflammatory responses;
- stimulation of various signaling cascades and production of cytokines;
- induction of apoptosis;
- cytotoxicity;
- mediation of cell proliferation;
- formation of oxidized macromolecule (including DNA) adducts; and
- induction of DNA strand breaks.

However, only the last two of the above list of ROS effects are potentially relevant to the initiation of cancer (the topic of this section). The other effects in the above list likely contribute to the induction of other asbestos-related diseases and may even promote (but not initiate) asbestos-related cancer. Thus, they are addressed further in later sections of this chapter (see below).

Although, ROS generation is associated with exposure to various particles and fibers (including all forms of asbestos), generation of ROS does not necessarily imply carcinogenesis. For example, Zhu et al. (1998) indicate that ROS generation is induced in response to exposure to asbestos, crystalline silica, and coal mine dust. However, based on an extensive record of human exposure, the latter (coal mine dust) is not carcinogenic in humans. Therefore, evidence related to the last two of ROS-associated effects listed above, are examined in more detail below.

Several studies indicate that, once generated by exposure to asbestos, ROS can interact with DNA *in vitro* and *in vivo* to produce oxygenated adducts, primarily 8-oxo-Guanine. Of the studies reviewed above, for example, Yamaguchi et al. (1999) observed that crocidolite, but not (non-tumorigenic) glass produced dose-dependent increases in 8-oxo-Guanine in rat lung tissue following intratracheal instillation. Also, Leanderson et al. (1988), Park and Aust (1998), Keane et al. (1999) indicate that asbestos induces formation of oxidized DNA adducts in *in vitro* assays. Brown et al. (1998) indicate that asbestos induces ROS-mediated DNA strand breaks.

However, not all DNA strand breaks attributable to asbestos occur through pathways involving ROS. Ollikainen et al. (1999) exposed cultures of human mesothelial cells (MeT-5A, transfected with SV-40, but nontumorigenic) to hydrogen peroxide (100 µM) or crocidolite (2–4 µg/cm²), either alone or in combination with TNF-α and performed assays for DNA strand breaks. The authors note that the concentrations of asbestos evaluated are well below those that have been associated with cytotoxic effects. Crocidolite alone was shown to produce DNA strand breaks at the concentrations tested. The authors also note that, at lower concentrations, only reversible effects were observed (presumably indicating DNA repair). Co-exposure to crocidolite and TNF-α increased the observed incidence of DNA damage, but the effect was less than additive. The authors indicate that additional studies with antioxidants indicate that the DNA damage induced by crocidolite in this study occurs through a mechanism that does not involve ROS. In fact, a potentially much more substantial mechanism by which asbestos may induce DNA breaks and various clastogenic alterations involves its ability to interfere with mitosis (Section 6.3.3.1).

There is also evidence that different tissues may respond to asbestos-induced ROS generation differently. For example, Zhu et al. (1998) indicate that MnSOD is found in the mitochondria of Type II epithelial cells of rats exposed to crocidolite. The authors further indicate that, because fibroblasts, alveolar macrophages, or endothelial cells do not display this protein when stimulated by exposure, this suggests a difference in the susceptibility of epithelial cells to certain types of asbestos-induced injury.

Importantly, although these studies provide evidence that indicates asbestos is capable of producing oxidized DNA adducts (or strand breaks) through ROS mediated processes, they do not address the question of whether such adducts can lead to heritable mutations in DNA *in vivo* nor do they indicate

whether such adducts lead to tumor production. Therefore, such studies should only be construed to suggest a potential that asbestos can act as a cancer initiator through ROS-mediated pathways.

As previously indicated, not all mechanisms involving the generation or effects of ROS are similarly fiber-size or fiber-type dependent and those that are do not necessarily depend on these variables in the same way. At this time, it is not possible to distinguish among the relative importance of the different mechanisms, so that it is difficult to judge the relative importance of the different effects. However, the overall general implication (with the few exceptions noted) is that ROS generation more likely contributes to other asbestos-related diseases and to cancer promotion than to cancer initiation.

One final note concerning the effects of ROS that specifically involves the behavior of the hydroxyl radical is also warranted. The hydroxyl radical is an extremely reactive species. Whether *in vitro* or *in vivo*, this species will react with virtually 100% efficiency with every organic molecule it encounters. Therefore the effects attributable to the hydroxyl radical are limited to those involving reactions in the immediate vicinity of the location at which it is generated. Thus, unless asbestos-induced generation of this radical occurs within the nucleus and in the immediate vicinity of susceptible strands of DNA, it is unlikely that these radicals are the direct cause of DNA damage.

Rather, hydroxyl radicals tend to react with cell membranes and other cellular components to produce further intermediate radicals (primarily lipid peroxides), which are much more stable than the hydroxyl radical and may migrate substantial distances before having an effect. It is likely that these intermediate radicals are ultimately responsible for any ROS-mediated DNA damage that may be attributed to asbestos.

6.3.3.3 Generation of reactive nitrogen species (RNS)

Nitric oxide (NO) is produced ubiquitously in biological systems and serves many functions (Zhu et al. 1998). It is highly reactive and, therefore, generally short-lived *in vivo*. However, nitric oxide has been shown to react with superoxide (O_2^-) to form the peroxy nitrite ion (ONOO $^-$) at near diffusion-limited rates (see, for example, Zhu et al. 1998). This the peroxy nitrite ion (an RNS) may represent the primary species responsible for the effects attributed to ROS (at least when the primary ROS formed is superoxide).

Asbestos-induced Generation of RNS. Alveolar macrophages, lung endothelial and epithelial cells, and alveolar epithelium (in both rats and humans), when stimulated by inflammatory agents, generate both superoxide and over-produce nitric oxide. These then combine to produce the peroxy nitrite ion (Martin et al. 1997; Zhu et al. 1998). These cells up-regulate production of NO when stimulated by various cytokines, lipopolysaccharide, and interferon γ . Because the peroxy nitrite ion is a strong oxidant and nitrating agent and is extremely reactive, evidence for its production is generally indicated in most studies by the presence of nitrotyrosine, the stable product of tyrosine nitration, (Zhu et al. 1998). Evidence for production of NO is frequently indicated by observation of nitrite. Numerous studies also provide evidence of nitric oxide and peroxy nitrite ion production specifically in response to exposure to asbestos in various tissues.

Both chrysotile and crocidolite up-regulate the production of nitric oxide by alveolar macrophages in the presence of interferon- γ and the interaction between asbestos and interferon is synergistic. Non-fibrogenic carbonyl iron did not induce nitric oxide formation (Zhu et al. 1998). These authors also cite a study in which intratracheal instillation of silica and coal mine dust caused more inflammation and nitric oxide formation than TiO_2 or carbonyl iron (on an equal particle basis). This suggests both the geometry and chemical composition of particles determine their ability to up-regulate nitric oxide.

Inhalation of chrysotile or crocidolite induces secretion of both TNF- α and nitric oxide by pleural macrophages (Tanaka et al. 1998). Tanaka et al. (1998) studied the effects of RNS in rats exposed by inhalation to 6 to 8 mg/m³ crocidolite or chrysotile (both NIEHS samples) for 6 hours/day, 5 days/week for 2 weeks. Rats were sacrificed at 1 and 6 weeks following exposure. The authors indicate that asbestos induces formation of stable products of nitric oxide in cells obtained by lung lavage 1 week after asbestos exposure. Nitrotyrosine (a marker for ONOO⁻ formation) was also observed. Also, a greater number of alveolar macrophages and pleural macrophages were shown to express iNOS protein (the inducible form of nitric oxide synthase, Table 6-6) than sham exposed animals. Exposed rats showed significantly elevated immuno-staining for nitrotyrosine in the region of thickened duct bifurcations as well as within bronchiolar epithelium, alveolar macrophages, and mesothelial cells of both the visceral and parietal pleura. Nitrotyrosine staining was persistent, being observed at both 1 and 6 weeks following exposure.

Quinlin et al. (1998) studied the production of nitric oxide in rats exposed to crocidolite or chrysotile asbestos (both NIESH reference samples). Rats were exposed by inhalation at 6 hours/day, 5 days/week and lavaged at 3, 9, and 20 days. Lavaged macrophages showed significantly increased nitrite/nitrate (indicating production of nitric oxide) and this was suppressed with inhibitors to iNOS. Thus, nitric oxide is produced via an iNOS pathway. The authors also note that nitric oxide production correlated temporally with neutrophil influx in the lavage fluid. They also indicate that asbestos exposed animals showed a 3- to 4-fold increase in iNOS positive macrophages in their lungs.

Quinlin et al. (1998) also exposed cultured murine alveolar macrophages (RAW 264.7 cells) to crocidolite, riebeckite, and cristobalite silica *in vitro*. These cells showed increased iNOS mRNA following exposure to asbestos and even greater increases if the cells were also stimulated with lipopolysaccharide (LPS). Both crocidolite and riebeckite (but not cristobalite silica) stimulated increased iNOS promoter activity when applied in combination with LPS. Thus, in this case, there appears to be a mechanism that is sensitive to particle composition, but not size.

Park and Aust (1998) treated cultures of human lung epithelial (A549) cells with crocidolite and observed induction of iNOS and reduction of intracellular glutathione (GSH) levels. Based on studies with inhibitors, the authors further indicate that iron mobilized from crocidolite was required both for formation of nitric oxide and to generate 2'-deoxy-7-hydro-8-oxoguanosine, but not for the observed decrease in intracellular glutathione. The authors note that approximately 5 times as much chrysotile (containing approximately 3% iron) as crocidolite was required to produce the same level of nitric oxide formation. Importantly, these experiments were conducted *in vitro* in serum-free medium, so that no extra-biological source of iron was present.

Choe et al. (1998) dosed cultured rat pleural mesothelial cells with either chrysotile or crocidolite (both NIEHS samples) at concentrations between 1.05 and 8.4 $\mu\text{g}/\text{cm}^2$ with or without co-stimulation with 50 ng/ml of interleukin-1 β (IL-1 β). The authors report that mRNA for iNOS in asbestos and IL-1 β dosed cells increased progressively from 2 to 12 hours following exposure. Both types of asbestos also stimulated production of nitric oxide (measured as nitrite) in IL-1 β stimulated cells in a dose- and time-dependent fashion. Both types of asbestos also induced expression of iNOS protein and formation of nitrotyrosine (based on nitrate detection) in IL stimulated cells. In contrast, carbonyl iron particles did not induce any of the effects observed for asbestos in IL stimulated cells. Thus, formation of RNS appears to be either fiber size dependent (not induced by particles) or mineralogy-dependent (or both).

As with the production of ROS, RNS production is apparently a function of multiple, complex mechanisms. Also, as with production of ROS, the dose-response characteristics of the various mechanisms differ. Several of the mechanisms show a strong dependence on fiber size and some dependence on fiber type. However, there are other mechanisms that are dependent primarily on fiber (or particle) type, but may not be dependent on size (or at least not dependent on fiber size). At this point in

time, it is not possible to gauge the relative importance of the various mechanisms by which RNS may be generated, except that it is likely that the importance of the various mechanisms likely differ in different cells and tissues and likely differ as a function of the specific toxin whose presence is inducing RNS production.

There are also indications that production of RNS may be (animal) species specific. For example, Jesch et al. (1997) report that alveolar macrophages harvested from rats expressed iNOS when stimulated with either LPS (lippopolysaccharide) or interferon- γ . In contrast, iNOS expression could not be induced in hamster, monkey or human macrophages.

Effects Mediated by RNS. Based on Zhu et al. (1998), over-production of nitric oxide can:

- inactivate critical enzymes;
- cause DNA strand breaks that result in activation of poly-ADP-ribosyl transferase (PARS);
- inhibit both DNA and protein synthesis; and
- form peroxynitrite by reaction with superoxide.

In turn, peroxynitrite ion may:

- initiate iron-dependent lipid peroxidation;
- oxidize thiols;
- damage the mitochondrial electron transport chain; and
- nitrate phenolics (including tyrosine).

Also, some of the damage to alveolar epithelium and pulmonary surfactant system previously attributed to reactive oxygen species may actually be caused through ROS generation of peroxynitrite. For example, Chao et al. (1996) report that crocidolite treatment of human lung epithelial cells (A549 cells) results in formation of 8-hydroxy-2'-deoxyguanosine (8-OHdG) in DNA and synthesis of mRNA for iNOS. An iNOS inhibitor reduces intracellular nitrite and eliminates production of 8-OHdG. Addition of independent NO donor, recovers production of 8-OHdG. Thus, production of the oxygenated DNA adduct in this case appears to be generated by reaction with RNS.

As with ROS, it is primarily the potential for RNS to contribute to DNA damage (e.g., strand breaks or generation of oxygenated adducts) that represent the primary pathways by which RNS might participate in cancer initiation (as opposed to cancer promotion or other asbestos-related diseases). It appears that RNS-mediated DNA damage is closely associated with ROS generation and mediation of DNA damage (see Section 6.3.3.2). Thus, there is little to add here.

6.3.3.4 *Conclusions concerning asbestos as a cancer initiator*

The strongest, most consistent evidence that asbestos can act as a cancer initiator relates to the tendency of asbestos to interfere with mitosis. Although there is evidence that asbestos may induce production of DNA adducts and DNA strand breaks (through ROS and RNS mediated pathways), whether such adducts or breaks ultimately lead to permanent, heritable changes to DNA remain to be demonstrated. The relative importance of the ROS/RNS mediated pathways compared to the pathway involving interference with mitosis also remains to be determined. As indicated in later sections, however, ROS/RNS mediated pathways may play substantial roles in cancer promotion and induction of other asbestos-related diseases.

Regarding the primary mechanism by which asbestos may initiate cancer (interference with mitosis), the pathway is length dependent (short fibers do not appear to contribute to the effect). Further, although

there may also be a dependence on fiber type (chemical composition), it is apparent that all types of asbestos can act through this pathway. The dependence of this pathway on fiber diameter is less clear. Thus, other than to suggest that fibers must be respirable (and therefore thinner than approximately 0.7 μm , Section 6.1) to have an opportunity to act, whether further diameter constraints are associated specifically with the mechanism of cancer initiation is not known.

For pathways involving generation of ROS or RNS, some mechanisms (such as those associated with frustrated phagocytosis) are length dependent, others are not. Although there appears to be some dependence on fiber type for several mechanisms and a general dependence of several of these mechanisms on surface chemistry, the relative importance of fiber type to the overall contributions from these pathways remains to be determined.

Importantly, although crystalline silica may also act to produce some of the same effects as asbestos (including potentially induction or promotion of cancer), there is substantial evidence that this material does not act through the same pathways and that the characteristics of its respective dose-response relationships may differ. Thus, for example, while asbestos likely initiates cancer through a mechanism that favors long (and potentially thin) fibers, silica more likely acts through a mechanism that is dependent on total surface area, with freshly and finely ground material likely being the most potent. In contrast, grinding asbestos fibers tends to lessen carcinogenicity overall. Due to differences in chemistry and crystallinity (reinforced by studies indicating a lack of correspondence in behavior) crystalline silica does not appear to be an appropriate analog for any of the asbestos types. Rather, for example, the appropriate non-fibrous analog for crocidolite is riebeckite and the appropriate non-fibrous analog for chrysotile is antigorite or lizardite.

There is also evidence that the relative importance of asbestos as a cancer initiator may differ in differing tissues. For example, asbestos can only interfere with mitosis in cells that actively phagocytize fibers and not all cell types actively phagocytize particles (although both mesothelial cells and pulmonary epithelial cells appear to actively phagocytize fibers, Section 6.3.3.1). However, there is also evidence that pulmonary epithelial cells (Type II) may undergo terminal differentiation to Type I cells and thus escape potential cancer initiation by asbestos (Section 6.3.3.1). Such a pathway is not available to mesothelial cells. To the extent that pathways involving generation of ROS or RNS contribute to cancer initiation, as indicated throughout this section, the rates of generation and the spectrum of the species generated varies as a function of cell type.

6.3.4 Evidence that Asbestos Acts As a Cancer Promoter

Primarily, asbestos may promote cancer by facilitating tissue proliferation. However, additional mechanisms associated with the observed interaction between asbestos exposure and smoking (Section 6.3.4.6) also need to be considered.

Substantial evidence exists indicating that asbestos induces proliferation in target tissues associated with lung cancer and mesothelioma and this is summarized below followed by an overview of studies that suggest the various mechanisms by which asbestos may facilitate such proliferation. Evidence suggesting the various mechanisms related to the interaction between smoking and asbestos exposure are also briefly reviewed.

There are numerous mechanisms by which asbestos may facilitate proliferation including:

- direct cell signaling to induce proliferation. This may occur by:
 - direct interactions between fibers and receptors on the cell surface;
 - interactions between phagocytized fibers and intracellular components of

- signaling cascades; and
- or interactions between cells and intermediate species (e.g., ROS or RNS) whose generation and release has been induced by asbestos; or
- response to induced cell death in target tissues, which then stimulates stem cells to proliferate to replace killed cells. Cell death may be induced either through:
 - inducing apoptosis (programmed cell death); or
 - direct cytotoxic effects, which leads to necrosis.

These pathways are summarized in Table 6-5, which provides a perspective on the complexity of the interactions between asbestos and the cells and tissues of the body.

Regarding asbestos-induced cell death, asbestos-induced apoptosis (and all of the other effects described above) typically occurs at exposure concentrations that are much lower than required to induce frank cytotoxic effects (Sections 6.3.4.3 and 6.3.4.4). Therefore, it is primarily the former that is of potential interest in terms of implications for asbestos-induced diseases in humans. Due to the high exposure concentrations typically required, the importance of contributions from frank cytotoxicity to human disease is unclear (Section 6.3.4.4).

6.3.4.1 Asbestos-induced proliferation

Numerous *in vivo* studies indicate that all types of asbestos induce proliferation in target tissues relevant to lung cancer and mesothelioma. Such proliferation is also suggested by the animal histopathological observations previously described (Section 6.2.2). Moreover, many of these studies suggest that the underlying mechanisms may be fiber size- and fiber-type specific. Responses may also be species-specific.

Importantly, there are some studies (primarily *in vitro* studies) that suggest asbestos acts to inhibit (rather than induce) proliferation. Although it is likely that the contrasting observations found in such studies are due to differences in conditions, timing, dose, or the type of asbestos employed, the underlying reason for the contrasting observations is not always apparent.

The evidence for proliferation is summarized by tissue below.

In lung epithelium. Brody et al. (1997) showed that rats and mice exposed for a brief (5 hour) period to chrysotile asbestos at 1,000 fibers/cm³ (no size indicated) exhibited focal scarring at bronchio-alveolar duct junctions that are identical to those seen in asbestos-exposed humans. After 3-consecutive exposures, the lesions persisted for 6 months. In regions where fibers are deposited, macrophages are observed to accumulate, epithelium is injured, and proliferation is observed to occur. In this study, the authors also showed by immunohybridization staining that the four genes required to express three peptide growth factors (TGF- α , TGF- β , and the A and B chains of PDGF) and the proteins themselves are expressed in bronchio-alveolar tissue within 24 hours of exposure. PDGF is expressed almost immediately and expression remains elevated for 2-weeks post-exposure, but only in regions where fibers are deposited.

The authors report that PDGF is a potent growth factor for mesenchymal cells, TGF- α is a potent mitogen for epithelial cells, and TGF- β inhibits fibroblast proliferation, but stimulates synthesis of extra-cellular matrix (Table 6-6). The authors also report additional experiments with knockout mice indicate that TNF- α is required to induce the early stages of proliferation. The authors also indicate that Type II cells produce TGF- β 1 and TGF- β 2 (two of three isoforms of this protein) and that they are stimulated to do so when co-cultured with macrophages.

Adamson (1997) intratracheally instilled size-separated (by sedimentation) long and short crocidolite fibers into rats (0.1 mg in a single dose) and noted that the long fibers damaged the bronchiolar epithelium and that fibers were incorporated into the resulting connective tissue; granulomas formed with giant cells containing fibers). The long fibers also appeared to escape into the interstitium. Labeled thymidine uptake (which indicates DNA synthesis and suggests proliferation) following long fiber exposure was seen in lung epithelial cells, fibroblasts, and pleural mesothelial cells. Such labeling peaked at 2% in mesothelial cells and 3% in epithelial cells within one week following exposure. Proliferation appeared to end shortly beyond one week. Short fibers were observed to have been efficiently phagocytized by alveolar macrophages and a small increase in macrophage population appeared to have been induced. Otherwise, none of the other effects attributable to long fibers (described above) were observed with short fibers. Note that such observations are entirely consistent with those reported for the range of studies described in Section 6.2.2.

McGavran et al. (1989) exposed both normal (C5+) mice and compliment deficient (C5-) mice to asbestos (at 4 mg/m³) by inhalation and observed proliferation of bronchio-alveolar epithelium and interstitial cells at alveolar duct bifurcations (based on incorporation of tritiated thymidine) between 19 and 72 hours after a single, 5-hour exposure. Sham exposed rats showed fewer than 1% of epithelial and interstitial cells at alveolar duct bifurcations incorporate labeled thymidine. In contrast, thymidine uptake in asbestos exposed animals is significantly elevated for the first few days, begins to decrease at 8 days, and returns to normal by one month following exposure. Both C5+ and C5- mice show similar increases in volume density of epithelial and interstitial cells at 48 hours post-exposure. However, one month following exposure C5+ mice developed fibrotic lesions while C5- mice were no different than controls. The authors conclude that the depressed macrophage response in C5- mice does not appear to change the early mitogenic (and proliferative) response to asbestos, but apparently attenuates later fibrogenesis.

Chang et al. (1989) describes the morphometric changes observed in rats following 1 hour inhalation exposure to chrysotile (at 13 mg/m³). Within 48 hours following exposure: the volume of the epithelium increased by 78% and the interstitium by 28% at alveolar duct bifurcations relative to sham-exposed animals. Alveolar macrophages increased 10-fold and interstitial macrophages 3-fold. Numbers of Type I and Type II epithelial cells increased by 82% and 29%, respectively. At 1 month following exposure, the numbers of Type I and Type II pneumocytes were still elevated, but not significantly. However, the volume of the interstitium had increased by 67% accompanied by persistently high numbers of interstitial macrophages, accumulation of myofibroblasts, smooth muscle cells, and an increased volume of interstitial matrix.

In lung endothelium. In addition to the general evidence for proliferation of epithelial cells provided by Adamson (1997), McGavran et al. (1989), and Chang et al. (1989), as cited above, a more detailed description of the nature of asbestos-induced proliferation of endothelial cells is also available.

Proliferation of endothelial cells and smooth muscle cells of arterioles and venules near alveolar duct bifurcations is induced in rats inhaling chrysotile (no size information given) for 5 hours at 4 mg/m³ (McGavran et al. 1990). This is based on the observed uptake of labeled thymidine (which indicates DNA synthesis and suggests proliferation) that is significantly increased over controls between 19 and 72 hours following exposure. Twenty-eight percent of vessels near bifurcations exhibited labeled cells 31 hours after exposure. One month following exposure, the thickness of the smooth muscle layers around these blood vessels is significantly increased (doubled). In contrast, labeling of these same endothelial and smooth muscle cells in sham exposed rats is zero. The authors indicate that endothelial cells and smooth muscles associated with pulmonary blood vessels are normally quiescent with turnover rates on the order of years.

In mesothelium. In the second part of the study addressing epithelial proliferation, Adamson (1997) reports that rats instilled with 0.5 mg of unmodified, UICC crocidolite were sacrificed at 1 week and 6 weeks following exposure and subjected to bronchiolar lavage and pleural cavity lavage. Lavaged alveolar macrophages were observed to contain fibers, but pleural macrophages did not. At 1 week, collected pleural macrophages were shown to induce proliferation of fresh mesothelial cells in culture and pleural lavage fluid showed an even greater effect. No effects were observed at 6 weeks. Further work with anti-bodies to various cytokines indicated that early, transient proliferation of mesothelial cells was dependent on keratinocyte growth factor (KGF), but not on PDGF, FGF, or TNF- α (Table 6-6). This suggests that early, transient proliferation is induced by diffusing cytokines rather than direct fiber exposure. Adamson further reports that KGF is a fibroblast-derived cytokine that acts on epithelial cells so that its up-regulation likely results from epithelial injury with penetration of asbestos to the interstitium (where fibroblasts are found, Section 4.4). A similar transient proliferative response in mesothelial cells was also observed following exposure to chrysotile and in response to crystalline silica exposure. Thus, it appears that the mesenchymal proliferative response may be mineralogy specific for particles and is size-specific for fibers.

Everitt et al. (1997) exposed rats and hamsters by inhalation to RCF-1 (45 mg/m³-650 f/cm³) for 12 weeks and then let them recover for up to an additional 12 weeks prior to sacrifice. The authors indicate that both rats and hamsters showed qualitatively similar levels of inflammation at time examined (4 weeks and 12 weeks). They also indicate the mesothelial cell proliferation was observed in both animal types, but was more pronounced in hamsters at all time points examined. The greatest proliferation in both species was in the parietal pleura lining the diaphragm. The authors also report that fibers (primarily short and thin) were also observed in the pleural cavities of both species at all time points.

Several *in vitro* studies provide evidence that asbestos either induces or inhibits proliferation in lung tissues of interest and that at least some of the mechanisms involved are fiber size and mineralogy dependent. As previously indicated, the specific reasons for the apparent contrast between results observed *in vivo* (where asbestos consistently promotes proliferation) and the inhibition sometimes observed in *in vitro* studies is not always apparent. However, it must be due to the special conditions that must be created to conduct *in vitro* studies, which may not support certain mechanisms that are important *in vivo*.

Timblin et al. (1998a) completed a study in which rat pleural mesothelioma (RPM) cells in culture were dosed with crocidolite or various cation-substituted erionites. The expression of several gene and gene products were then tracked. Cultures in this study were exposed to 1, 5, or 10 μ g/cm² of the various fibrous materials. Analysis of the fibrous materials indicated that crocidolite contained many more fibers per gram of material (probably because they are thinner) and that the preparation contains somewhat longer fibers than the erionites evaluated. In crocidolite, for example, 88% of the fibers are longer than 5 μ m, 68% longer than 10 μ m, and 37.5% longer than 20 μ m. All of the cation substituted erionites showed approximately the same size distribution: 50% longer than 5 μ m, 10–20% longer than 10 μ m, and 1–5% longer than 20 μ m.

Results indicate that the various cation substituted erionites behave differently and that the Na substituted erionite shows the largest overall potency, at least for some endpoints, but not others. Fe, Na, and Ca substituted erionite all appear to induce c-fos expression in a dose-dependent fashion (increasing regularly among the 1, 5, and 10 μ g applications). K-erionite may also show the same pattern, but the changes were not indicated as significant over controls (apparently due to greater variability). Only Na-erionite showed significantly increased expression of c-jun (at 1 and 5 μ g applications, but not significantly at 10 μ g, apparently due to greater variability. However, the mean result for 10 μ g shows a consistent trend with the lower concentration application results).

Na-erionite induces c-fos at the same or greater rates as crocidolite asbestos for the same mass application (but not the same fiber number). Crocidolite also appears to show a dose-response trend for c-jun expression, but only the result for the highest application (10 µg) is significantly different from controls. In contrast, Na-erionite appears to show greater induction of c-jun expression at lower dose than crocidolite, but the increase with increasing dose is much lower for Na-erionite. Crocidolite also appears to induce substantial apoptosis (even at the low dose of 5 µg) and that the induction is dose-dependent. In contrast, non-fibrous riebeckite does not appear to induce apoptosis. Comparison between crocidolite dosed cultures and Na-erionite dosed cultures indicate that crocidolite induces substantial apoptosis at all time periods following application, but that Na-erionite induces little apoptosis even at higher mass dose and longer time periods than crocidolite. The authors also indicate that crocidolite and Na-erionite appear to stimulate DNA-synthesis, which appears to be a compensating mechanism to fiber cell toxicity. The authors indicate that chemistry is important in fiber toxicity as Na-erionite was a strong inducer of c-jun, even at relatively low concentrations, but several of the other cation substituted erionites (including Fe-erionite) were not. They further suggest that, given the difference in the fiber lengths of the crocidolite samples and Na-erionite samples, that fiber length may be a less important consideration than fiber surface chemistry. However, despite the author's assertion, considering that non-fibrous riebeckite does not induce any of the effects observed for crocidolite, there appears to be a clear size effect. It may simply require that a defined, minimum length is necessary to induce the effect.

The authors also indicate that balance between proliferation and apoptosis is required to maintain homeostasis in healthy tissue. They further indicate that other studies suggest that c-Jun expression is linked to proliferation and induction of cancer, while c-fos expression is linked to apoptosis. Thus, suppression of c-fos may be linked to carcinogenesis by allowing establishment or maintenance of a transformed cellular phenotype. This is in fact an early step in carcinogenesis. Many environmental agents stimulate both apoptosis and proliferation and, depending on the degree, may cause imbalances that lead to disease. Relative stimulation of c-fos and c-jun may reflect some of these pathways. Since crocidolite induces both c-fos and c-jun in this study, the implication is that it mediates both apoptosis and proliferation.

Wylie et al. (1997) dosed hamster tracheal epithelial (HTE) cells and rat pleural mesothelial (RPM) cells with various asbestos and talc samples and evaluated proliferation based on a colony-forming efficiency (CFE) assay. The samples were NIEHS crocidolite and chrysotile and three different talcs. Samples were characterized in the paper by mineralogical composition, surface area, and size distributions.

The authors indicate that both asbestos samples increased colony formation of HTE cells (suggesting induction of proliferation), but talc samples did not. RPM cells, in contrast, showed only dose-dependent decreases in colony forming efficiency for all samples, which the authors indicate is a sign of cytotoxicity. The authors report that all samples show corresponding effects when concentrations are expressed as fibers longer than 5 µm or by total surface area. They also suggest that the "unique" proliferative response by HTE cells could not be explained by either fiber dimension or surface area and suggests a mineralogical effect.

Barchowsky et al. (1997) dosed cultured (low passage) endothelial cells to NIEHS chrysotile, crocidolite, or RCF-1. After 1 to 3 hours exposure to 5 µg/cm² (non-lethal concentrations), asbestos (but not RCF-1) causes changes in cell morphology (cells elongate), increases in cell motility, and increases in gene expression. Further work by the authors indicate that these effects are mediated by interaction between asbestos and the receptor for urokinase-type plasminogen activator (uPAR). The authors also suggest that attachment of asbestos to cell membranes, internalization of asbestos fibers by the cells, and the morphological changes induced by asbestos are each mediated by different proteins:

Examples of *in vitro* studies that indicate asbestos (and other fibrous materials) may inhibit proliferation in culture include the following.